Scholars' Mine

1959

Mechanization of first stage graphitization in Fe- C-Si- alloys

Dildar S. Gill

MECHANISM OF FIRST STAGE GRAPHITIZATION

IN Fe- C- Si- ALLOYS

BY

DILDAR S. GILL

———————

A

THESIS

submitted to the faculty of the

SCHOOL OF MINES AND METALLURGY OF THE UNIVERSITY OF MISSOURI

in partial fulfillment of the work required for the

Degree of

MASTER OF SCIENCE IN METALLURGICAL ENGINEERING

Rolla, Missouri

1959

———————

Approved by

_____
Advisor

_____

_____

_____

ACKNOWLEDGMENTS

CONTENTS

LIST OF ILLUSTRATIONS.

LIST OF TABLES

INTRODUCTION

The art of imparting a certain amount of ductility and toughness to castings made originally of white cast iron and, therefore, extremely hard and brittle, is a very old one. The operation consists of a long annealing of the castings at a temperature well above their thermal critical ranges, followed by very slow cooling. The article now known as "Black Heart" castings are made up of many rounded particles of temper carbon embedded in a matrix of ferrite.

Considerable research has been carried out on the graphitization of binary (iron-carbon) and ternary (iron-carbon-silicon) alloys. The kinetics of graphitization in these alloys and the effect of manganese and sulphur ratio on the morphology of graphite nodules has been thoroughly investigated. The effect of various alloying elements on the kinetics of graphitization has been fully studied, but the role of alloying elements is not yet fully understood.

The heterogenous nucleation of graphite nodules is still largely unexplained in quantitative terms. However, the problems surrounding the mechanism of growth of the nodules are well understood. The controlling mechanism is the rate of solution of carbides.

The mechanism of graphitization was generally thought to be well explained until the publication of a paper by Taub[1] in October, 1958. He criticised the old theory that temper car-

---

[1] All references are in bibliography.

bon precipitates directly from the supersaturated austenite.
With the help of a few micrographs, he indicated that second-
ary globular carbides precipitate from the austenite, which
later decompose into temper carbon and carbon depleted austen-
ite.

Purpose of Investigation:

The purpose of this investigation was to study the mech-
anism of first stage graphitization in iron-carbon-silicon al-
loys in the light of results obtained by Taub, and to propose
a new mechanism of graphitization. The results of preliminary
experiments confirmed the findings of Taub as regards the pre-
cipitation of secondary carbides. Therefore, it was decided
to extend the investigation so as to include the study of
growth of secondary carbides. In order to know the chief
factor responsible for the growth of secondary carbides, the
activation energy was calculated. Another factor which was
investigated was the site of graphite nuclei formation.

Plan of Investigation:

Only the early stages of graphitization were investigated,
as the mechanism of graphite nodule growth has already been
thoroughly worked out. The dilation method was employed to
determine the degree of graphitization. The metallographic
studies were made to investigate the precipitation of second-
ary carbides and to locate the sites of graphite nuclei forma-
tion.

Dilatometer specimens were prepared from the iron-carbon-
silicon alloy, and these were chromium plated to avoid oxida-

tion and decarburization. The specimens were annealed at various temperatures by moving the already hot furnace of the dilatometer over the specimens. Specimens were held at various temperatures for different periods of time and then were water quenched. The change in length of the specimens was noted, and it was assumed to be proportional to the degree of graphitization. The specimens were fractured and transverse sections were prepared for microscopic examination. The growth of secondary carbides was studied under the microscope and the activation energy was calculated from the growth rate.

REVIEW OF LITERATURE

In 1722 Reaumur, a French Physicist, described a process for producing malleable cast iron by packing small castings of white cast iron in pulverised hematite ore and heating them to bright redness for many days. H is product was the so called "White Heart" malleable in which carbon was completely removed. The art of making "Black Heart" malleable iron was discovered in America probably unconciously by Seth Boyden while attempting to practice Reaumer's method in 1826.

Boyden and others who were concerned with the production of malleable iron were manufacturers rather than scientists and probably for this reason no papers were published and the production of malleable iron castings remained a closely guarded secret for about one hundred years. This undoubtedly was the cause of the retarded development of the theory of the process.

The pioneer work in putting the process on a scientific basis was conducted in 1875 by Hammer[2]. He found it possible to lay down "a chemical ratio as between carbon and silicon, and manganese and sulphur". His conclusions were thought to be too valuable trade secrets to warrant publication. At the same time Pope[3] came to similar conclusions with reference to manganese and sulphur ratio.

Sauveur[4] published his first rudimentary iron-carbon diagram in 1896, which indicated various transformations and phase regions. In 1902, Charpy and Grenet[5] published a paper on graphitization of white cast iron. Howe[6], in 1908 discussed

critically and exhaustively the evidence then available on graphitization. In 1910, Moldenke[7] published a book outlining his knowledge and experience in the malleablization technique. In the same year, Hatfield[8] discussed the chemical physics of the precipitation of free carbon from iron carbon alloys. In 1911 Ruff and Goecke[9] published a study of the solubility of carbon in iron and in the same year Ruer and Iljin[10] discussed the stable system of iron-carbon.

The first scientific American contribution to the literature of the metallurgy of malleable iron was a publication of the results of some research work dealing with the fundamentals of the graphitizing reaction by Storey[11] in 1913. Archer, White, Merica and Schwartz were very active in malleable iron research during the early 20's. In 1919, Merica[12] stated that cementite in white cast iron decomposed at temperatures between 700° and 1000°C producing temper carbon. He also indicated that the elements which promoted graphitization by lowering the temperature range within which the decomposition of cementite is possible during annealing of white iron, were the same which promote graphitization upon solidification.

In 1920, Honda and Murakami[13] advanced the theory that graphitization does not take place directly but is consequent of oxidation by CO_2 and subsequent decompositon of CO formed with liberation of free carbon. There appears to be little doubt, however, that although graphitization may be accelerated by this gas as by a catalyst, graphitization of cementite can, nevertheless, proceed without it. Thus, Pingault[14] re-

ported fairly rapid graphitization of cementite in a vacuum at temperatures above 1000°C.

Bain's[15] work demonstrated fairly definitely that graphitization may take place from austenite and cementite simultaneously. Philips and Davenport[16] submitted micrographs that indicate that in ordinary annealing of white cast iron, temper carbon is formed directly from the solid solution areas, and not in general from the massive cementite areas.

In 1924, Hayes and Diederich[17] summarized all the theories in an informative bulletin. They outlined the theory that throughout the temperature range employed for first stage graphitization, cementite is metastable; the saturation limit in gamma iron of carbon derived from carbide is greater than the saturation limit of carbon derived from carbon. The carbide saturation line lies to the right of the carbon saturation line as shown in figure 1. Upon heating a white cast iron above the critical range, the pearlite is converted to austenite in which is dispersed much massive carbide. Upon soaking at annealing temperature, this carbide goes in solution in the austenite until the austenite is saturated with carbon from carbide. At this stage, it is supersaturated with respect to carbon from carbon and as a result carbon is deposited. Graphitization always starts at the surface of carbide particles because supersaturation is first attained there. The solution of carbide and the deposition of graphite continues until all the free carbide has disappeared and then deposition of graphite continues until the equilibrium concentration of carbon from the carbon for the temperature
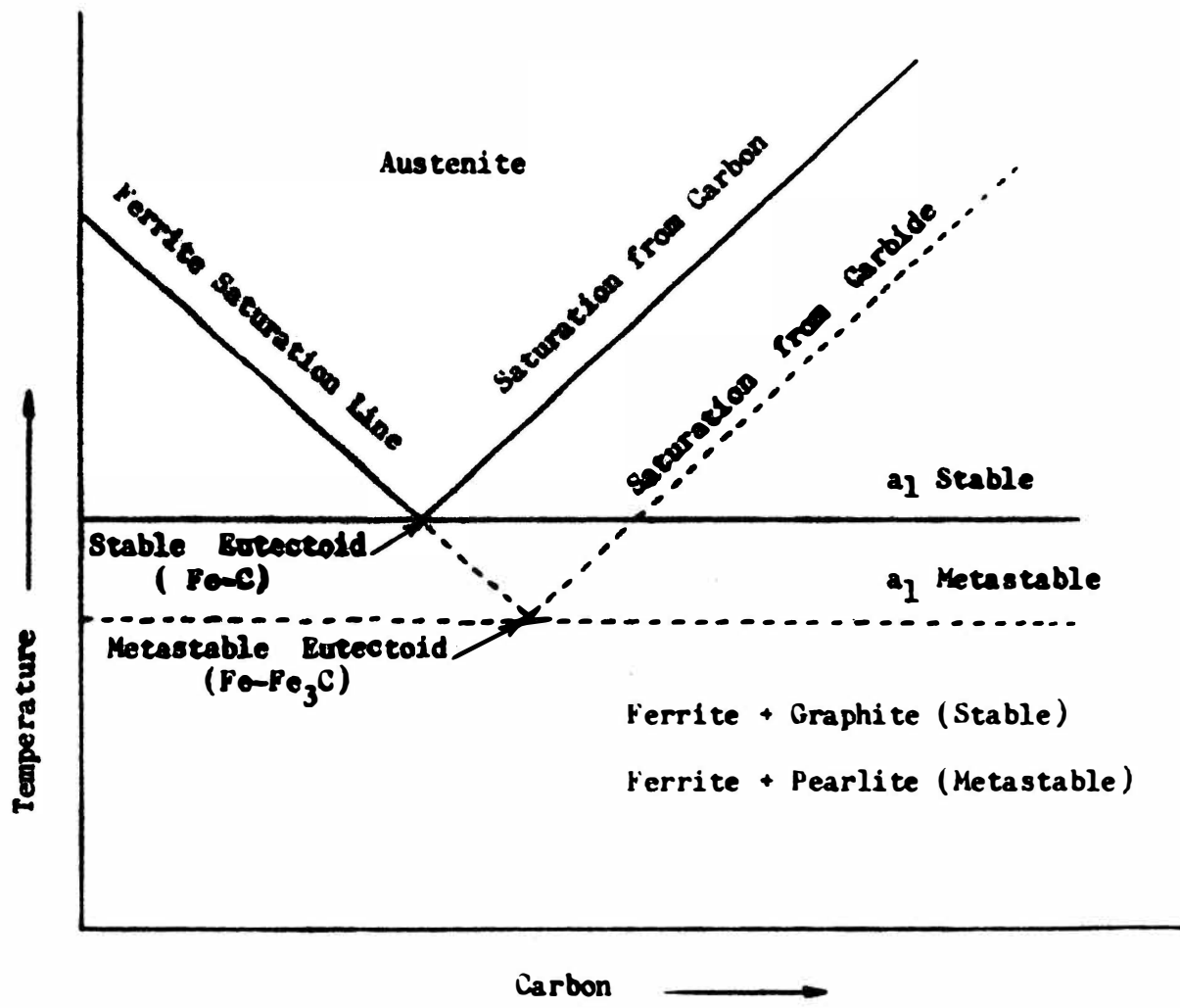
Figure 1 - A PART OF IRON-IRON CARBIDE AND IRON-GRAPHITE DIAGRAM. (Not to Scale)

is attained.

In 1928, Schwartz[18] claimed that the nucleation of graphite is probably due to inhomogeneties of stress or composition. The presence of graphite nuclei acts as a powerful aid to graphitization. Bain[19] suggested that once graphite forms it means the presence of an additional phase and, therefore, according to the phase rule a decrease in the degree of variance of the system. This would tend to accelerate the disappearance of one of the phases, namely cementite.

Yap[20], on thermodynamic grounds, concluded that cementite is unstable at low temperatures, but becomes more stable at higher temperatures, and above 940°C is thermodynamically stable. His work was later disputed by Schwartz[21] and Chipman[22]. It was definitely proved by Wells[23] that cementite can be decomposed to graphite at any temperature between 700° and 1125 °C.

In 1935, Sauveur and Anthony[24] stated that free cementite only graphitizes above the thermal critical range. The carbon present in the austenite matrix above that range must be thrown out of solid solution before graphitizing can take place.

Much interest was aroused in the 30's among investigators in what constitutes a nucleus of a graphite nodule. Schwartz[25], on the basis of the micrographs presented by Junge, stated that secondary graphitization customarily begins at a cementite-solid solution interface. In non-eutectiferous iron-carbon-silicon alloys in which such interfaces may not exist, the graphite is commonly seen to grow about manganese sulphide inclusions. In 1936, Schwartz and Ruff[26] expressed the opinion

that the nucleus of a graphite nodule may be a submicroscopic fragment of graphite or of metallic oxide or silicate, or only a field of force due to surface tension at an interface. It was further stated that there might be any one or more of these nuclei even in the same metal.

In 1938, Wells[27] presented a classic paper on the graphitization of iron carbon alloys. He determined the equilibrium iron-graphite diagram in the vicinity of the eutectoid. He demonstrated that graphite forms directly from austenite and as a decomposition product of cementite. The graphite from solution occurs in former austenite grain boundaries, possibly at austenite-carbide interfaces, and as spherical masses. Graphite from carbide appears to form along crystallographic planes in carbide masses, in possible cracks of the brittle carbide, and as approximately spherical masses. Schwartz[28] stated in 1942 that the form of the isothermal time-graphite curve can be predicted given a sufficient knowledge of the various fundamental constants. He gave an elaborate mathematical treatment for calculation of values of time for various stages of completion of the graphitization process by various reactions.

At the symposium on graphitization held in 1942 Schwartz[29] summarized his views with regard to the mechanism of graphitization. He repeated his conjecture that a graphite nodule grows around an oxide or sulphide particle that has been rejected at the surface of a cementite grain. He also discussed the film theory of graphitizing retardation.

McMillan[30] stated in his paper presented at the symposium

that the number of graphite nodules is greater in the higher
silicon irons and that with continued heating at the same
temperature the number of graphite nodules decrease.

In 1949, Zener[31] gave an analytical expression for the
rate of growth of a spherical particle growing in a matrix
originally of uniform composition. Brown and Hawkes[32] modified
and applied Zener's approach specifically to cast iron and
published a comprehensive paper on the kinetics of graphitiza-
tion of cast iron in 1951. According to Brown and Hawkes,
the process of decomposition of cementite above the eutectoid
temperature is one in which graphite nuclei form, and carbon
atoms diffuse through austenite to precipitate on the grow-
ing graphite particles; during the reaction the iron atoms of
cementite attach themselves to the adjacent austenite lattice.
Further, it was reported that the morphology of the graphite
thus produced is controlled by the composition of the alloy
and by the temperature of the reaction. It was noted that
the carbide particles nearest to the nodule dissolved faster
than those somewhat more remote. It was stated that in gen-
eral the growth rate increased with increasing temperature.
In one of their experiments, the growth rate was observed to
be discontinuous, which they explained on the basis that the
growth rate is an algebraic sum of the effects of diffusion
and competitive nucleation. Brown and Hawkes postulated that
if carbide-austenite was the principal site of nucleation,
then the probability of nucleation will be a function of the
total carbide-austenite interfacial area, which for a given
carbon content depends upon carbide size distribution. They

supported the view held by McMillam[33] and other investigators that at a given temperature the number of nodules reach a maximum and then decrease with increasing time. They explained this on the basis that the solution potential of carbon at the surface of nodules of small diameter is greater than that at the surface of nodules of larger diameter. They also stated that the rate of nucleation and growth are increased by increasing the temperature.

In 1954, Burke and Owen[34] determined the isothermal reaction rate curves by measuring the length changes of the specimen. It was observed that the time of the completion of the first stage of graphitization and the incubation period (on logarithmic scale) are approximately linear functions of temperature, and the two lines are approximately parallel. It was further noted that although variation in silicon content alters the position, it has no effect on the slope of the linear plot. The average value of the slope was found to be - 0.010.

Burke and Own indicated that their data can be examined by using the semi-emperical equation:

$$y = 1-\exp (t/k)^n$$

where y is the fraction transformed at time t, k is a temperature dependent rate constant. The average value of n is equal to 4.07. They gave a value of 68000 cal/mole for the activation energy of graphitization.

According to Burke and Owen the growth of graphite nodules in iron-carbon-silicon alloys involve three diffusion processes. They pictured diffusing carbon as an advancing in-

terface against which silicon will build up. For carbon dif-
fusion to continue, silicon must diffuse away. Iron atoms
must also diffuse away from the centers of nucleation in order
to provide free volume for the growing graphite. It was not-
ed that rate of growth is controlled by the rate of silicon
diffusion although the possibility of iron diffusion govern-
ing the rate was not discounted. They were of the opinion
that the influence of temperature on the rate of nucleation
is greater than its influence on the rate of growth.

On the basis of extensive experimental evidence, Hultgren
and Ostberg[35] concluded that the effect of increased S: Mn
ratio and/or increased hydrogen content of the surrounding
atmosphere was to increase the compactness of the aggregates
and to change the shape of the graphite units forming those
aggregates into equi-axed particles. They also stated that
favored nucleation sites for graphite were found to be iron
sulphide or manganese sulphide on the one hand and austenite
or cementite on the other.

In 1958, Taub[1] refuted all the mechanisms proposed previ-
ously and with the help of micrographs proposed that the pro-
cess of graphitization occured in two steps. First, the sec-
ondary globular carbides were precipitated from austenite, and
then these carbides decomposed into graphite and carbon de-
pleted austenite.

Role of Alloying Elements:

In answer to the query whether graphitization will take
place in absence of such elements as silicon, Schwartz[36] stat-

ed that graphitization is a phenomenon occuring in binary al-
loys of as high a purity as is obtainable. However, silicon
plays such an important role in the graphitization of iron-
carbon alloys that it must be dealt with in any discussion of
the mechanism of graphitization.

Silicon is known to promote graphitization in cast iron,
but the mechanism of this action is not very clearly under-
stood. Wust and Peterson[37] and Becker[38] found that increas-
ing the silicon content reduced the solubility of carbon in
cast iron and lowered the percentage of carbon in the eutectic.
As graphitization generally increases with increasing carbon
content, there may possibly be a connection between this ef-
fect of silicon and its tendency to promote graphitization.
According to Hatfield[39] some of the silicon in cast iron is
present in the iron carbide; the amount in the carbide increas-
ing with the silicon content. He considered the silicon con-
tent in the carbide to be responsible for the varying degree
of stability of that constituent.

In 1942, Schwartz[40] listed the elements, silicon, alumin-
ium, titanium, zirconium, nickel, copper, and uranium, which
definitely accelerate the graphitizing rate when present in
not too great a quantity. On the other hand, manganese, chro-
mium, molybednum, vanadium and tungsten retard the grahiti-
zation rate. He did not put forward any theory to explain
the effect of various elements on the graphitization rate.

Brown and Hawkes[41] held the view that the elements which
affect the graphitizing rate of white cast iron, do so prima-
rily through their effect on the stability of cementite. Using

the model of cementite lattice as proposed by Austin[42], they suggested that the elements nickel and cobalt, which enter the lattice, thus distending it, make the cementite less stable. On the other hand, atoms like chromium, which enter the lattice causing it to contract, make the cementite become more stable. Also certain elements which enter the lattice interstitially cause the cementite to become more stable, presumably by forming with the carbon some subsidiary bonding reinforcing the existing resonance bonding. Although, Brown and Hawkes present no experimental eveidence, they point out several points in favor of the theory, i. e. that certain deoxidizers, Aluminium, Boron, and Manganese act as graphitizers in small quantities and stabilizers in quantities in excess of the amount needed for deoxidation.

Burke and Owen[43] indicated that increasing silicon content markedly increases nucleation rate and also slightly increases rate of growth.

DISCUSSION OF MECHANISM OF GRAPHITIZATION

The ferritic "Black Heart" castings are made up of many rounded particles of temper carbon in a matrix of ferrite. The transformation of white iron into finished malleable iron is accomplished in two stages. The first stage consists in converting the cementite-pearlite structure into austenite and graphite by a long annealing of the casting well above its thermal critical range. The second stage of the process is the formation of ferrite and graphite which is usually accomplished by slow cooling through the critical range. Some of the more recent concepts of first stage malleabilization are discussed in the following short resume.

A glance at a micrograph showing graphite nests in malleable cast iron clearly indicates that temper carbon is not arranged like the cementite in the original white cast iron, and that graphitization has not taken place in situ. The conclusion that may be drawn is that the migration or diffusion of carbon takes place through the solid solution, with subsequent precipitation of carbon from solid solution onto the existing graphite nuclei.

It was pointed out by Schwartz[44] that graphitization process can be split up into the solution of cementite, its dissociation, the migration of carbon and its deposition. The rate of graphitization will be governed by the slowest of the four enumerated processes under existing circumstances. These several processes may not be similarly affected by changes of temperature and composition. It was stated by Schwartz that

for an extremely short period in the beginning the rate is determined by the crystallization velocity of graphite. For most of the deposition of graphite, it is governed by the rate of migration of carbon. In the end, the dissociation rate is the controlling factor. The dominant importance of carbon diffusion has been fairly conclusively ruled out by the observations of Wells, Batz and Mehl[45]. It was stated by Burke and Owen[46] that besides the migration rate of carbon, the diffusion of iron and silicon should be considered for studying the rate of graphitization of iron-carbon-silicon alloys. They observed that the rate of silicon diffusion governs the rate of growth, although the possibility of iron diffusion controlling the rate was not ruled out.

In view of the recent disclosure by Taub[1] of secondary carbide preciptation, it seems necessary to include the precipitation rate of secondary carbides and their decomposition as the variables to be considered for studying the rate of graphitization.

The graphite nodule formation has been well established as a process of nucleation and growth. It is believed that the nuclei for graphitization can be present in the "as cast" white iron. The number of nuclei increase with increase in the annealing temperature. Also at a given temperature, the number of nodules reach a maximum and then decrease with increasing time. This indicates that nuclei can be precipitated and redissolved.

As graphite nodules are found at the austenite-cementite

interfaces, it is assumed that the graphite nuclei form at these interfaces. There is no conclusive microscopic proof to substantiate this statement. It is, however, indirectly verified by the fact that quenched iron, which has a large cementite-austenite interfacial area, graphitizes very rapidly. The very fine carbides produced by tempering would tend to form a large interfacial area and thus tend to increase the grahitization rate.

Graphitization rate is known to be affected by temperature and chemical composition. The percent reaction vs. reaction time (on log scale) curves were plotted by Brown and Hawkes[47] for different temperatures and chemical compositions. It was observed that all the curves were similar in shape as shown in figure 2, and the curves could be superimposed by simple lateral shifting of the log time axis. This was also confirmed by Burke and Owen[48].

The role of alloying elements on graphitization is not well established. Many observers have stated that those elements which form stable carbides retard graphitization. In case of Chromium and Manganese the retardation may be through this action. But this theory does not account for the behaviour of other elements like Titanium and Silicon. It was reported by Schwartz[49] that carbide in malleable iron has silicon associated with it. Silicon being a weak carbide former, would tend to make the cementite more unstable. But it has been shown by Owen[50] that silicon is not present in the cementite lattice, and thus its effect cannot be explained on the
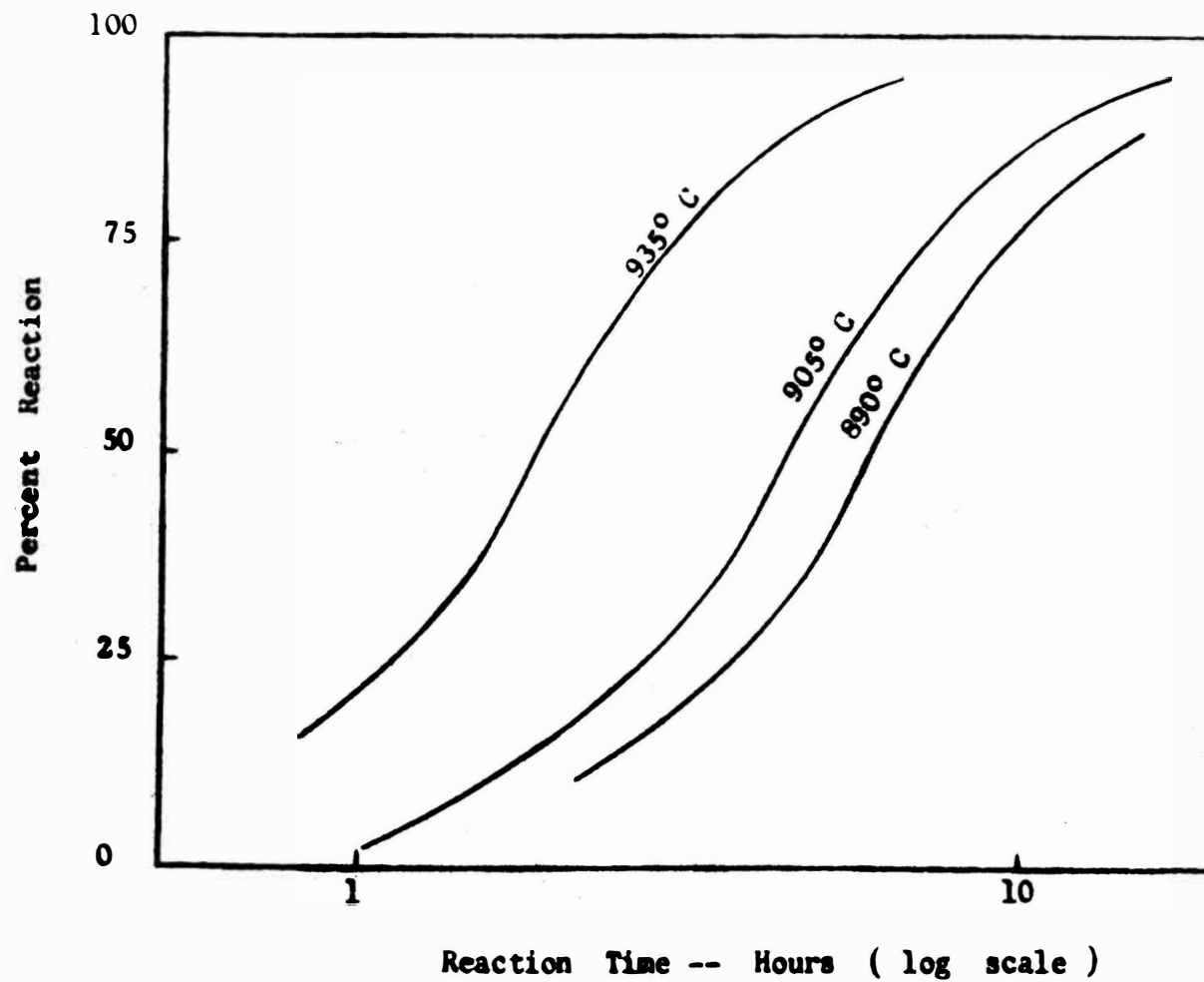
Figure 2 - GAMMA RANGE GRAPHITIZATION REACTION CURVES FOR
2.35 % C, 0.98 Si and 0.17 % Mo ALLOY.

(Brown and Hawkes)

basis of carbide unstability.

The fact that many of the elements which are graphitizers are strong deoxidizers, has led to considerable speculation that their effect is due to the fact that they have removed oxygen. There is no reason to believe that Nickel or Copper could act in this way. On the other hand, Manganese, which is rather powerful deoxidizer, is a retarder of graphitization.

All the theories proposed for the role of alloying elements are oversimplified and alloying elements may have some other additional means, of affecting the graphitization rate, by affecting the diffusion rate of carbon or iron atoms in the austeuite.

In conclusion it can be noted that the old theories for the mechanism of graphitization should be modified as to include the precipitation of secondary carbides as proposed by Taub. The role of alloying elements is not well understood and there is a vast field for research on this subject.

EXPERIMENTAL TECHNIQUES AND RESULTS
Preparation of White Cast Iron

Two 1500 gm. heats of iron-carbon-silicon alloy of a slightly different composition were prepared in the high frequency furnace. The photograph and the specifications of the high frequency furnace are given on page 21. The constituent elements used in the investigation were Armco iron, ferro silicon and electrode carbon. The chemical analysis of these materials is given in Table I.

Armco iron was first melted in a silica crucible. When the iron was in a liquid state, small quantities of carbon and ferro silicon were added simultaneously. When these went into solution, fresh additions were made until the iron contained requisite amounts of carbon and silicon. The complete charge of the two heats is given in Table II.

The ingots used in the experiment were produced by casting the iron-carbon-silicon alloy into a 3/4 inch diameter and 15 inch long dry graphite mould. The compositions of the ingots are given in Table III.

As the number of dilatometer specimens which could be prepared was limited, it was decided to conduct the experiments only on heat No. 1.
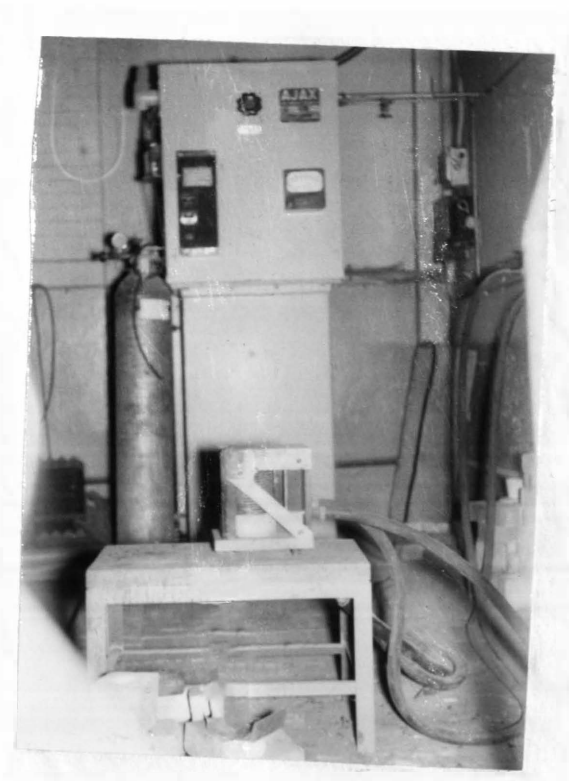
Figure 3

HIGH FREQUENCY INDUCTION FURNACE

TABLE I

COMPOSTION OF MATERIALS

Element	Armco Iron	Ferro-silicon
Carbon %	0.012	1.0 max.
Manganese %	0.017	-
Phosphorus %	0.005	0.04 max.
Sulphur %	0.025	0.04 max.
Silicon %	Trace	80-85

TABLE II

AMOUNTS OF MATERIALS

Material	Heat No. 1	Heat No. 2
Armco Iron	1500 gms.	1500 gms.
Electrode Carbon	45 gms.	50 gms.
Ferro-silicon	33 gms.	36 gms.

TABLE III

COMPOSITION OF THE INGOTS

Element	Ingot No. 1	Ingot No. 2
Carbon %	2.45	2.74
Silicon %	1.45	1.57

PREPARATION OF DILATOMETER SPECIMENS

The degree of graphitization was determined by measuring length changes in a differential optical dilatometer. $1-\frac{1}{2}$ inch long pieces were cut from the 15 inch long ingot with the carborundum cut off wheel. A number of pieces were examined under the microscope to make sure that no slag inclusions were present. To minimize the possible effect of small variations in grain size across the section each piece was split longitudinally into quadrants, and the dilatometer specimens were ground out of each quarter. The dilatometer specimen was 5 mm in diameter and 25 mm in length. A great care was excercised in cutting and in preparation of specimens so as not to over heat the material.

ELECTROPEATING OF DILATOMETER SPECIMENS

In order to avoid oxidation and decarburization of the specimens at high temperatures, it was decided to electroplate the specimens with either nickel or chromium. Electroplating was preferred over working in a vacuum or maintaining an inert atmosphere because of its simplicity.

Nickel plating with a copper base was first tried. The specimens were severely oxidized in about 3 hours at 800° C. The specimens were then plated with 0.001 inch thick chromium plating. The specimens did not oxidize at 925° C even after 5 hours.

The following procedure was adopted to obtain pore proof chromium plating.*

1. The specimens were weighed.

2. The specimens were cleaned in a weak alkali solution and then rinsed with distilled water.

3. The specimens were dipped in a 5% H_2SO_4 solution to remove the last traces of alkali solution.

4. The specimens were rinsed with distilled water and kept immersed in water until ready to plate.

5. The specimens were mounted on the copper rod cathode and sheet lead anodes were put in place. Two sheet lead anodes, one on either side of the specimens, were used because of the low throwing power of chromium.

6. The current is switched on and the CrO_3 solution is poured

---

* Please see acknowledgements

in the cell to cover the specimens.

7. The specimens were plated at a current density of 2 amps/sq. inch for 50 minutes; the specimens were reversed and plated for 50 minutes more.

8. The specimens were washed, dried and weighed. The gain in weight was noted.

9. The thickness of the plating was calculated from the gain in weight.

The composition of the electrolyte is given in Table IV, and the working conditions are listed in Table V.

TABLE IV

COMPOSITION OF THE ELECTROLYTE FOR CHROMIUM PLATING

CrO_3............... 240 gms./Litre
K_2SO_4.............. 3.7 gms./Litre
Cr^{VI}/SO_4.......... 60/1

TABLE V

CHROMIUM ELECTROPLATING WORKING CONDITIONS DATA

The specimens were electroplated in two batches of 12 and 16 specimens each.

	Batch I	Batch II
No. of specimens	12	16
Weight of bare specimens	22.012 gms.	28.851 gms.
Weight of plated specimens	22.450 gms.	29.412 gms.
Gain in weight	0.438 gms.	0.561 gms.
Approximate thickness of chromium plating	0.001 in.	0.001 in.
Total Voltage	6.0 volts	7.5 volts
Total Current	9.5 amp.	12.5 amp.
Current Density	2.0 amp/in^2	2.0 amp/in^2
Total time of electroplating	100 minutes	100 minutes

DILATOMETER STUDIES

The study of graphitization rates can be made by employing any of the following methods, each of which has some inherent disadvantage.

1. ## Chemical Analysis Method:

Frequently graphitization does not occur with such uniformity that sample, weighing one gram, can be considered as representing what has gone on as the average of a large piece. Therefore, it is often necessary to analyse many samples in order to obtain a usable average.

2. ## Measurement of Expansion Method:

The liberation of carbon results in the expansion of the specimen which can be measured. The chief advantage of such a method is that information is obtained concerning a rather large volume of metal. This method has been used by several investigators to study the rate of graphitization but it is doubtful whether an exansion of the specimen is directly proportional to the percentage of the graphite formed, as assumed by these investigators.

3. ## Electric Resistance and Coercive Force Measurement:

Measurements of electric resistance and coercive force have been used similarly but are still more doubtful in interpretation.

4. ## Metallographic Methods:

On the assumption that the microscope will resolve part-

icles of graphite or cementite too small to be detected by the chemist, several investigators have adopted the metallographic technique for the recognition of the beginning or the end of the graphitizing process. However, when very few such particles exist, the liklihood that any of these few will appear in the polished surface becomes very small, thus reducing the precision of the technique.

In the present study expansion of the specimen was used to know the degree of graphitization while metallographic technique was adopted to determine the location of the graphite nuclei and for the study of the secondary carbides.

The degree of graphitization was determined by measuring length changes in a differential optical dilatometer. The details of the dilatometer are given in figure 4. The increase in length of the specimen was taken to be directly proportional to the degree of graphitization. A fully graphitized specimen was used as a standard. It was possible to detect length changes of 0.0002 inch. An electric resistance furnace was used to heat the specimens. The temperature of the furnace was controlled with the help of a rheostat and the variation of temperature within the working range was $\pm 5^\circ$ C. The temperature of the specimen was measured by placing a caliberated Pt/Pt-RH thermocouple near the test specimen, and noting the reading of the galvanometer supplied with the furnace. The accuracy of temperature measurement was $\pm 2.5^\circ$ C.

Before starting each experiment, the furnace was allowed to run for two hours after it had attained the temperature to
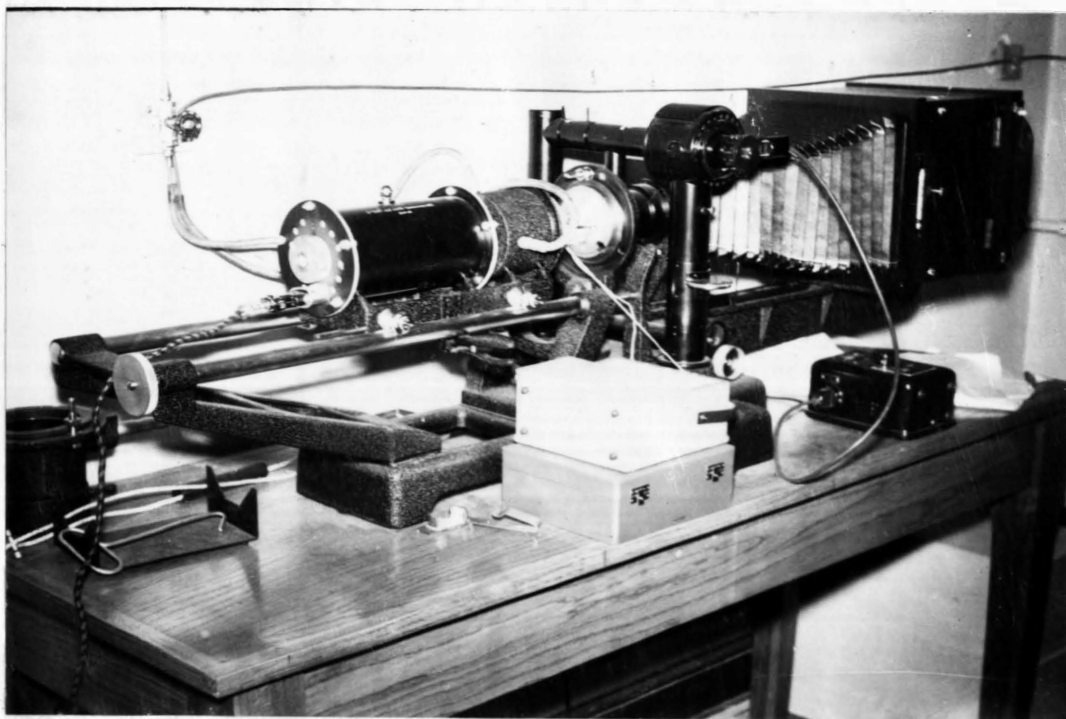
FIGURE 4

LEITZ OPTICAL DILATOMETER

establish equilibrium conditions. It took about two minutes to raise the temperature of the specimen from room temperature to the furnace temperature. In order to have some zero reference point for time, the time was measured after two minutes from the instant the furnace was moved over the specimen. The specimens were water quenched from the annealing temperature (800° to 925° C). The results of dilatometer investigation are given in Table VI.

It is evident from the expansion results that the incubation period is shorter at high temperatures. The maximum expansion, which corresponds to the total graphitization at the temperature, is more at lower temperatures. This is to be expected, as at high temperatures austenite requires a greater amount of carbon for saturation, and the amount of carbon held in solid solution in gamma iron is not available for graphitization.

TABLE VI

VALUES OF THE EXPANSION OF DILATOMETER SPECIMEN

Time in mts.	Expansion x 3.125 x 10^{-4}, inches at				
	800° C	825° C	875° C	900° C	925° C
20	Nil	Nil	Nil	Nil	Nil
40	Nil	Nil	Nil	2.5	5.0
80	Nil	Nill	1.0	14.0	20.0
160	Nil	Nil	6.0	26.0	27.0
320	1.0	2.0	32.0	-	-
640	9.5	-	-	-	-

PREPARATION OF SPECIMENS FOR METALLOGRAPHIC EXAMINATION

The specimens were fractured after annealing and the transverse sections were mounted in bakelite. The mounted specimens were ground on carborundum paper of 320 and 600 grit. The rough polishing was done on the wheel using diamond powder while the final polishing was done using the alundum powder.

The specimens were etched with 4% picral. The specimens were repolished and etched, and examined under the microscope. Repolishing was done to remove the disturbed layer formed during first grinding and polishing.

Photomicrographs were taken on the Bausch and Lomb metallograph at a magnification of 1000x. Micrographs taken are attached on the following pages.

Micrograph No. 1   Sample as cast   1000 x
Picral Etch.

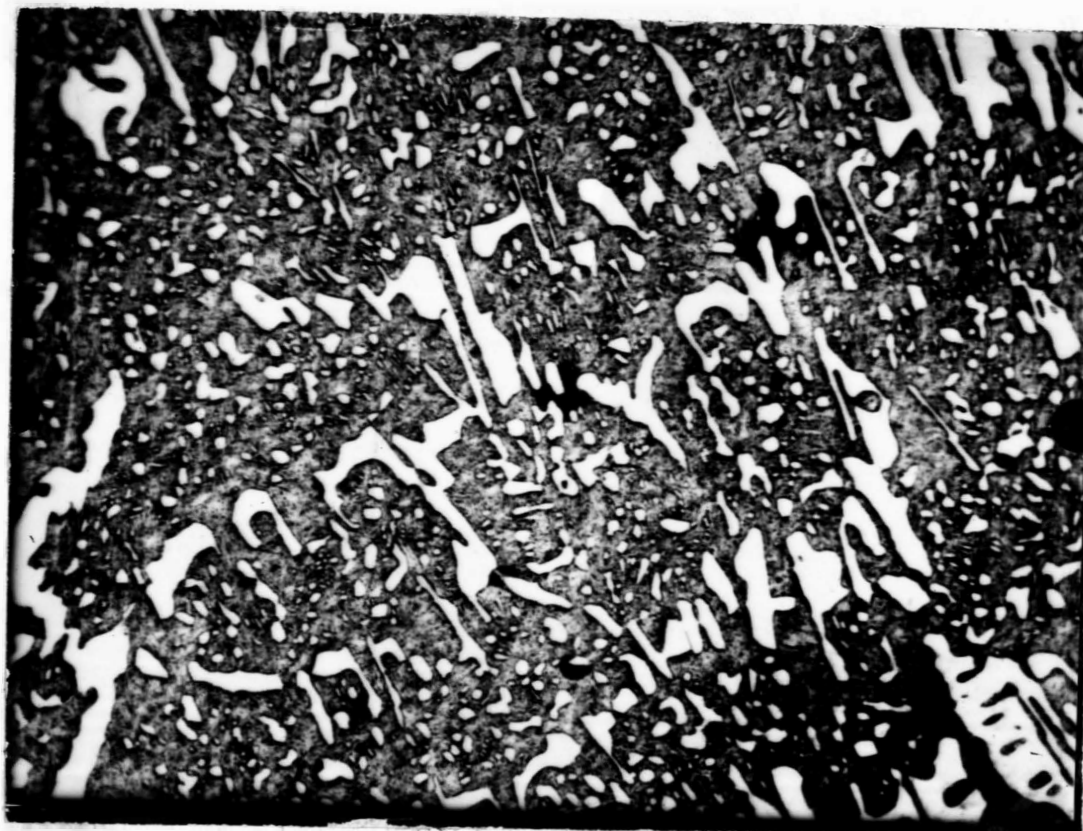No. 2   Annealed at 800° C for 20 minutes

1000 x

Picral Etch.

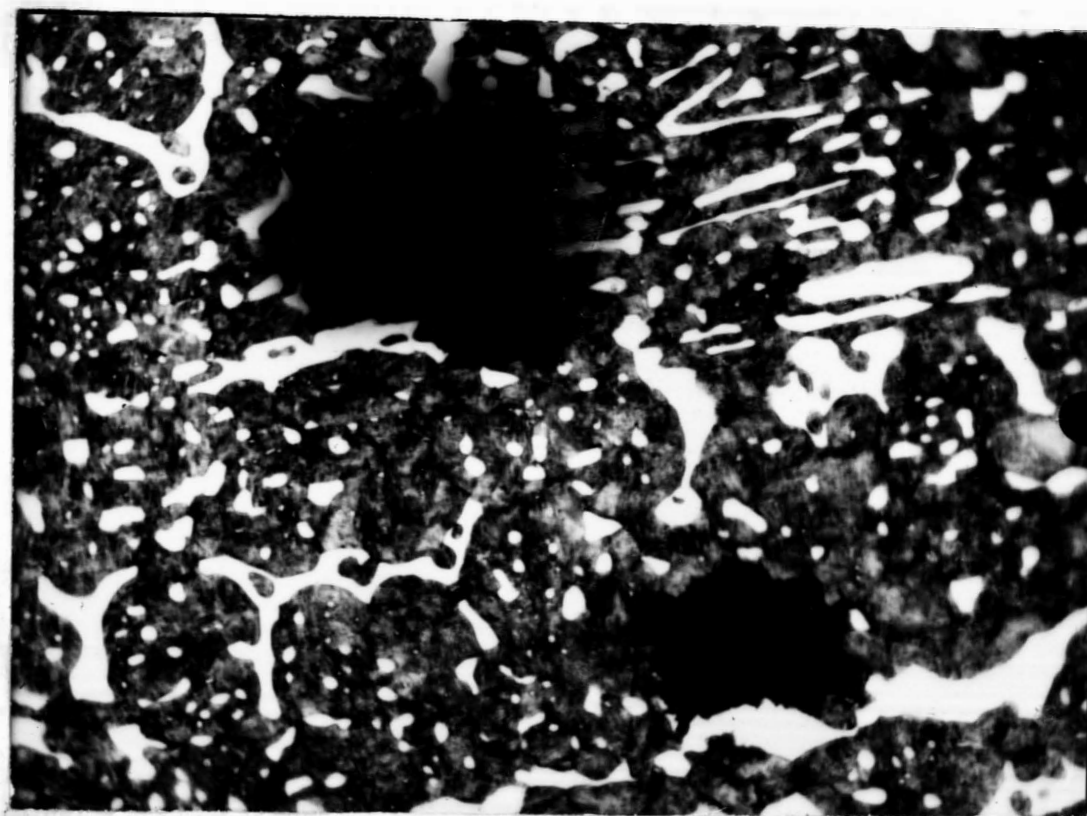No. 3   Annealed at 800°C for 40 minutes 1000 x
Picral Etch.
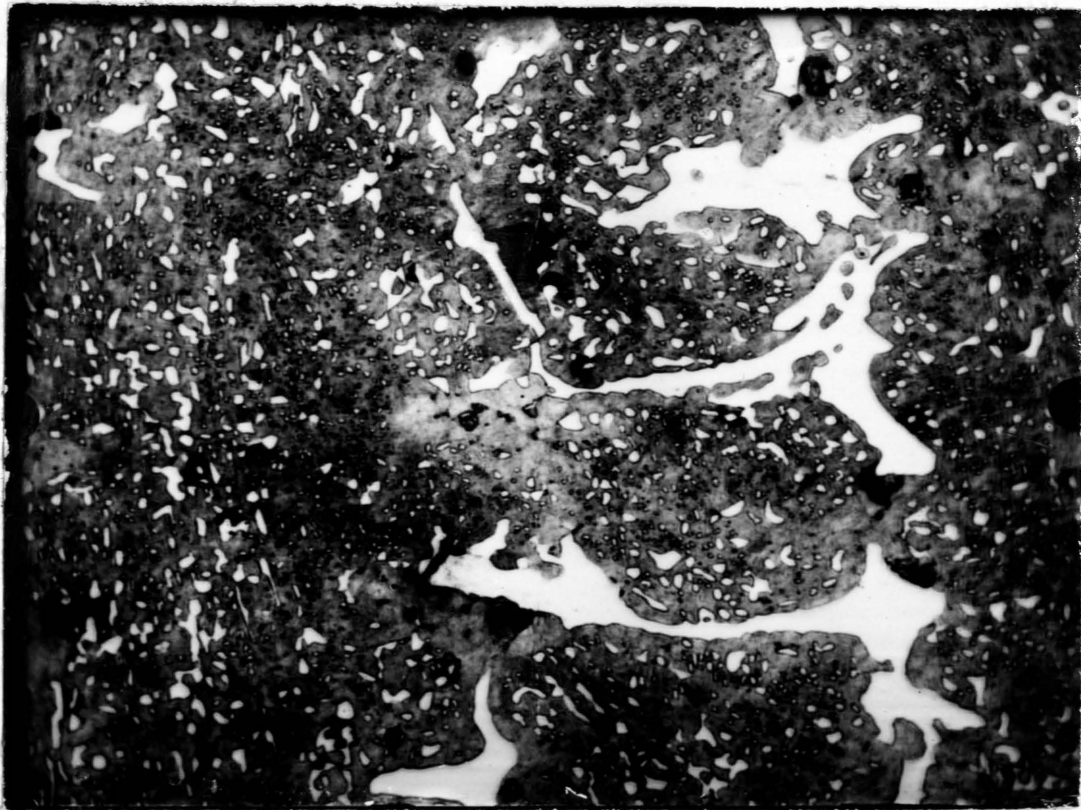
No.4   Annealed at 800° C for 80 minutes 1000 x
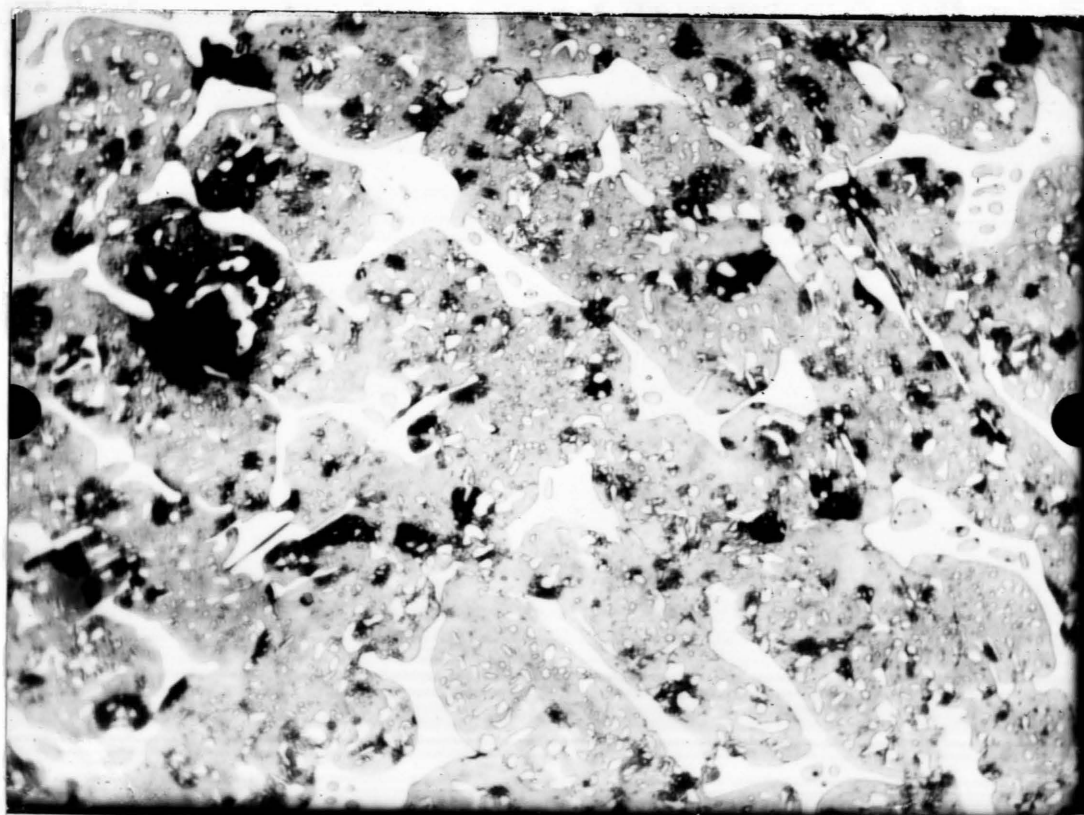
Picral Etch.

No. 5   Annealed at 800° C for 160 minutes   1000 x
Picral Etch.
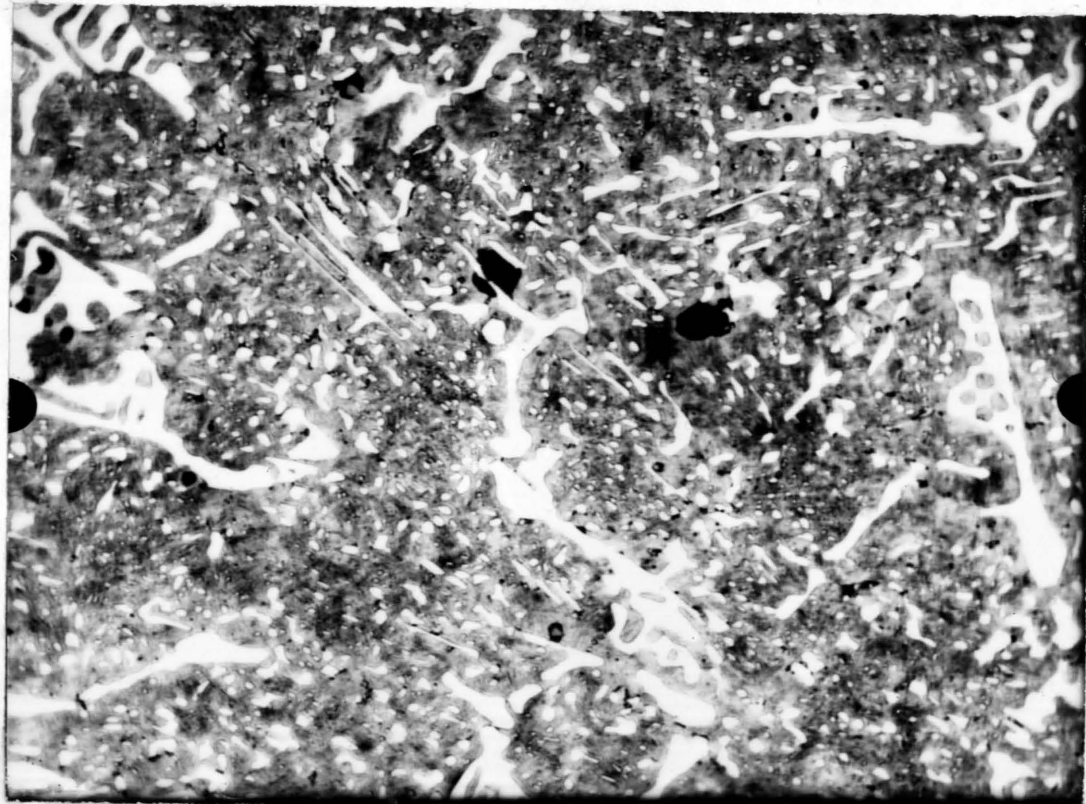
No. 6   Annealed at 800° C for 320 minutes   1000 x
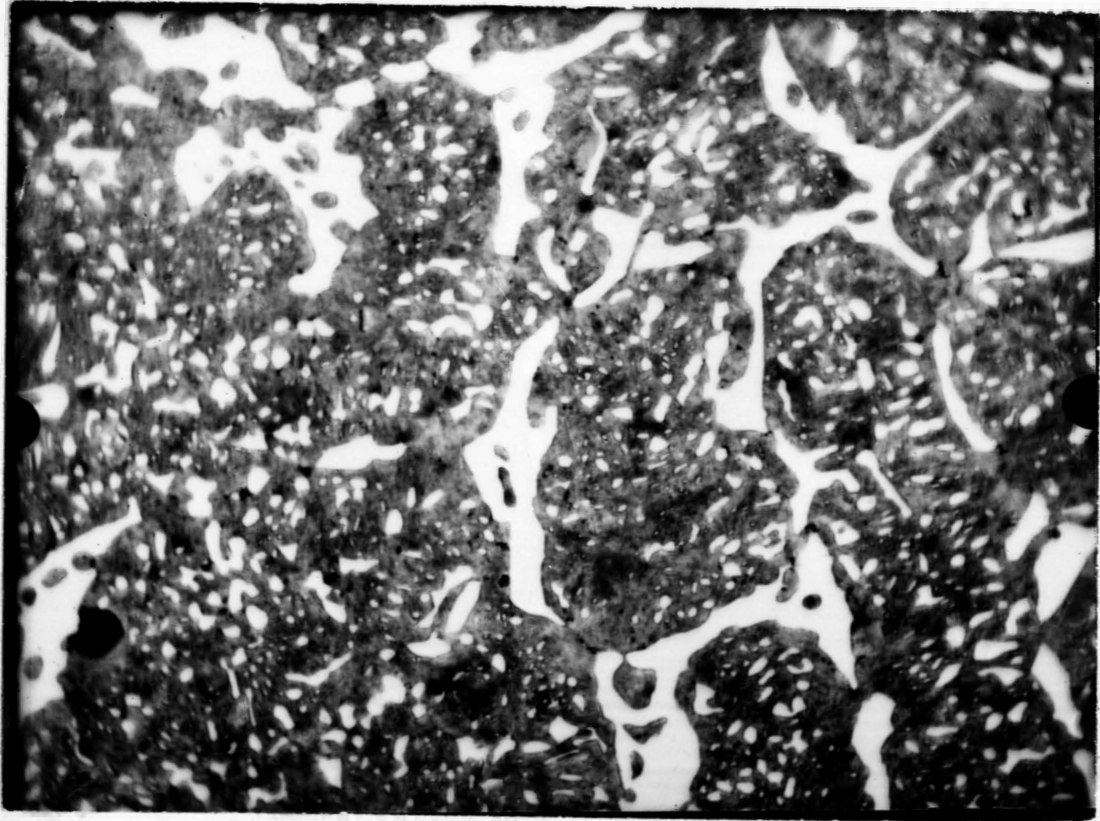Picral Etch.

No. 7   Annealed at 800° C for 640 minutes   1000 x
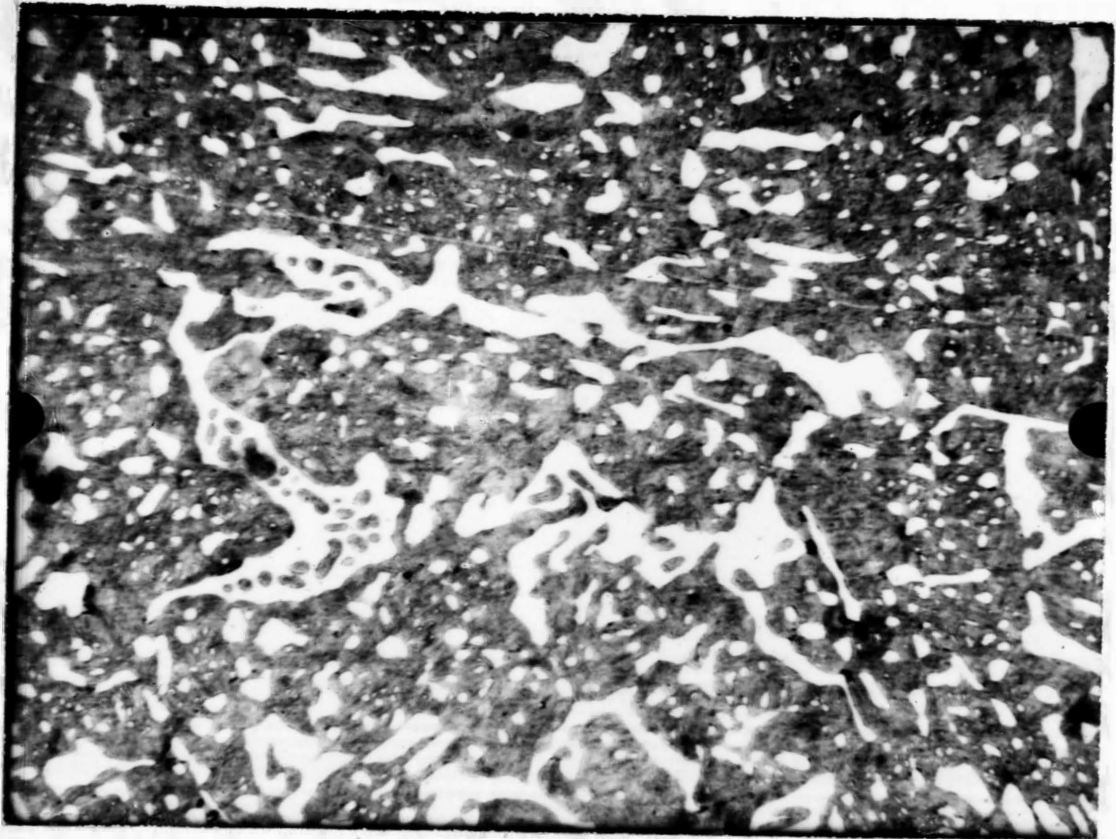
Picral Etch.

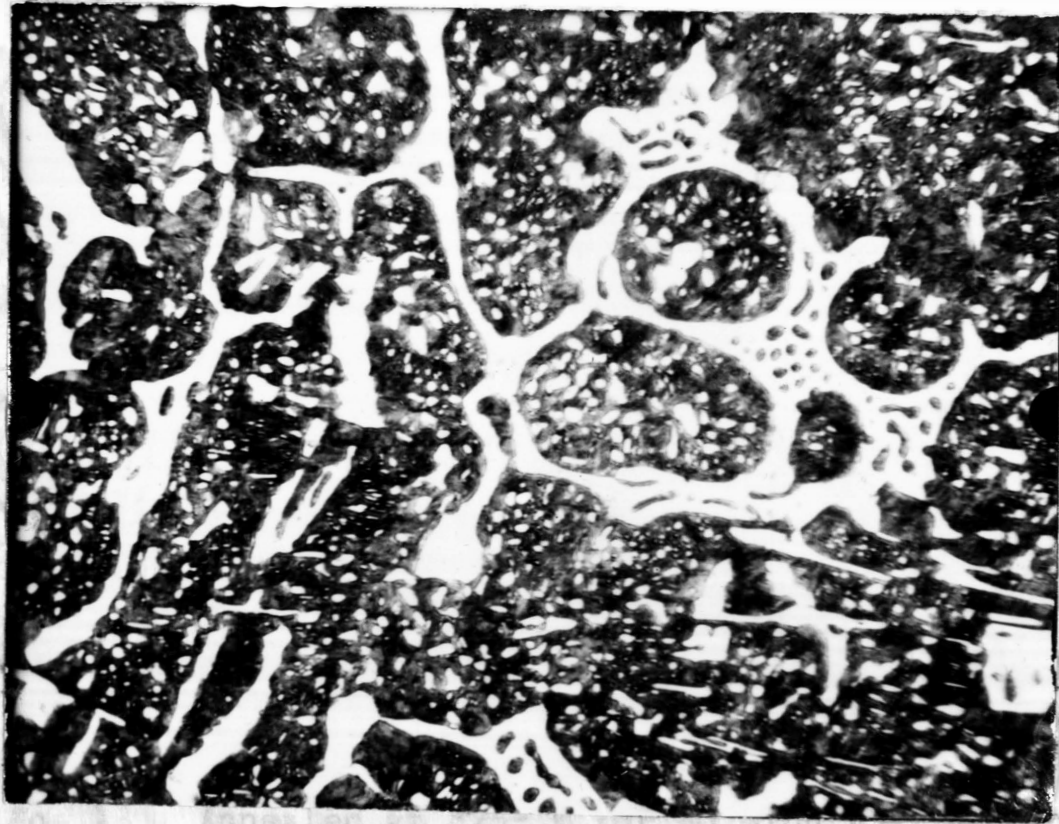No. 8   Annealed at 825° C for 40 minutes   1000 x

Picral Etch.

No. 9   Annealed at 825° C for 80 minutes   1000 x

Picral Etch.
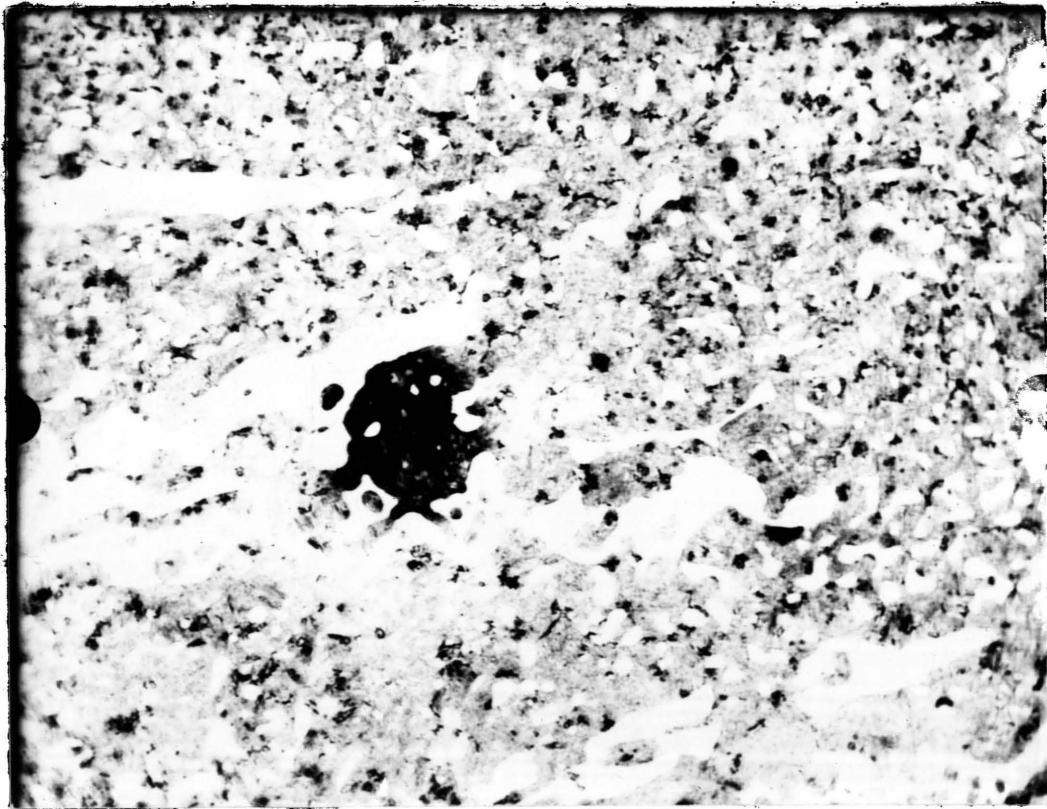
No. 10   Annealed at 825° C for 160 minutes   1000 x
Picral Etch.

No. 11   Annealed at 825° C for 320 minutes   1000 x
Picral Etch.

No. 12   Annealed at 875° C for 40 minutes   1000 x

Picral Etch.

No. 13   Annealed at 875° C for 80 minutes   1000 x

Picral Etch.

No. 14   Annealed at 875° C for 160 minutes   1000 x

Picral Etch.

No. 15   Annealed at 875° C for 320 minutes   1000 x

Picral Etch.

No. 16   Annealed at 900° C for 5 minutes   1000 x

Picral Etch.

No. 17   Annealed at 900° C for 20 minutes   1000 x
Picral Etch.

No. 18   Annealed at 900° C for 10 minutes   1000 x

Picral   Etch.

No. 19   Annealed at 900° C for 40 minutes   1000 x
Picral Etch.

No. 20   Annealed at 900° C for 80 minutes   1000 x

Picral Etch.

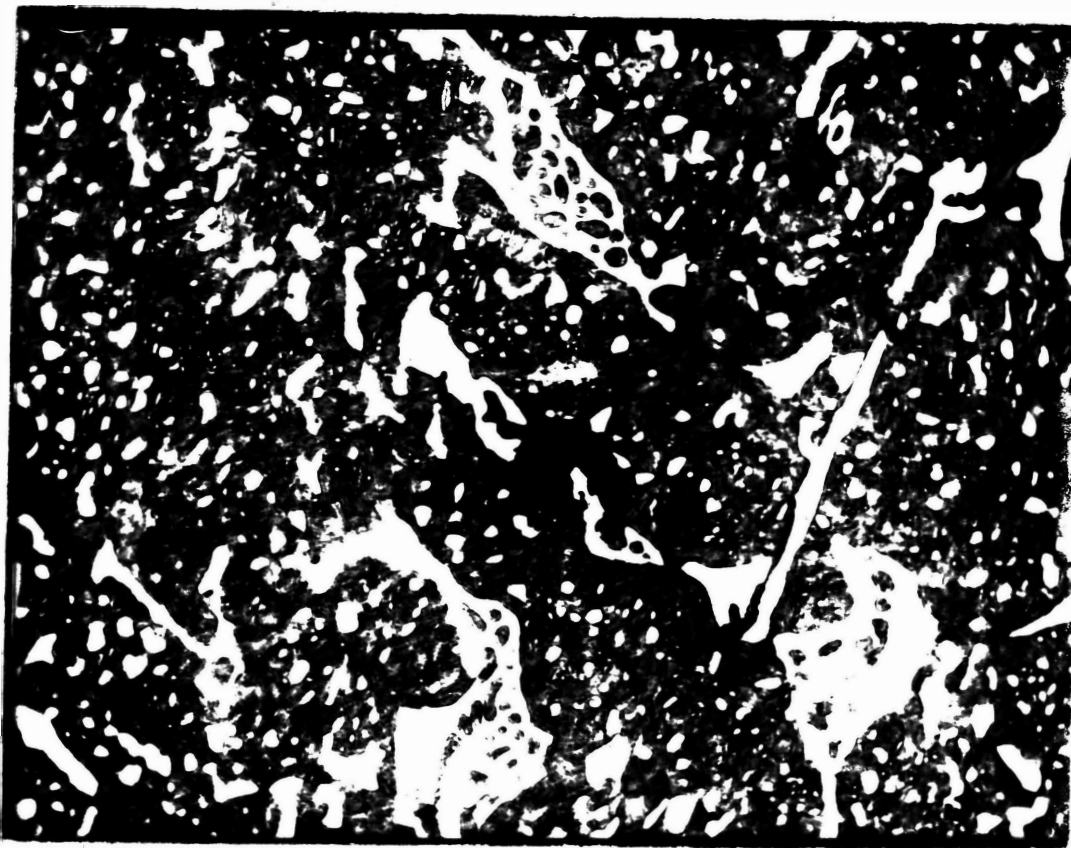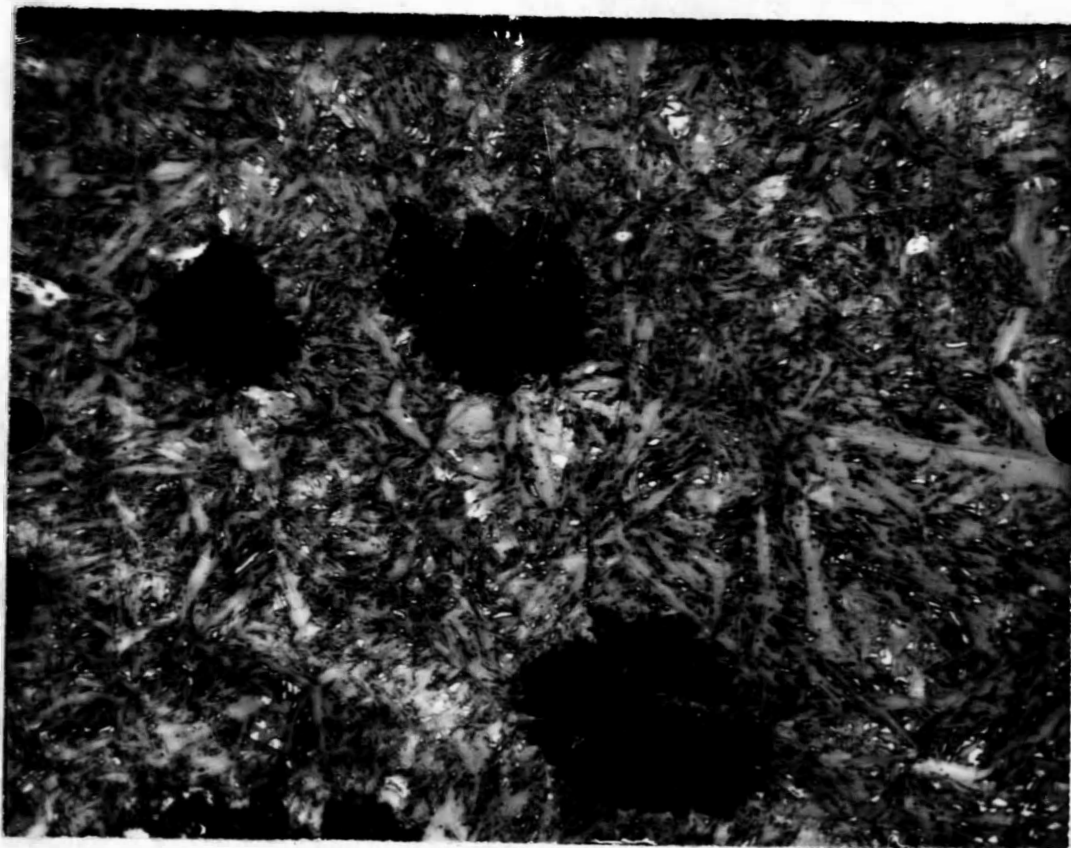No. 21   Annealed at 900° C for 160 minutes   1000 x

Picral Etch.

No. 22   Annealed at 925° C for 5 minutes   1000 x

Picral   Etch.

No. 23   Annealed at 925° C for 10 minutes

No. 24   Annealed at 925° C for 20 minutes   1000 x
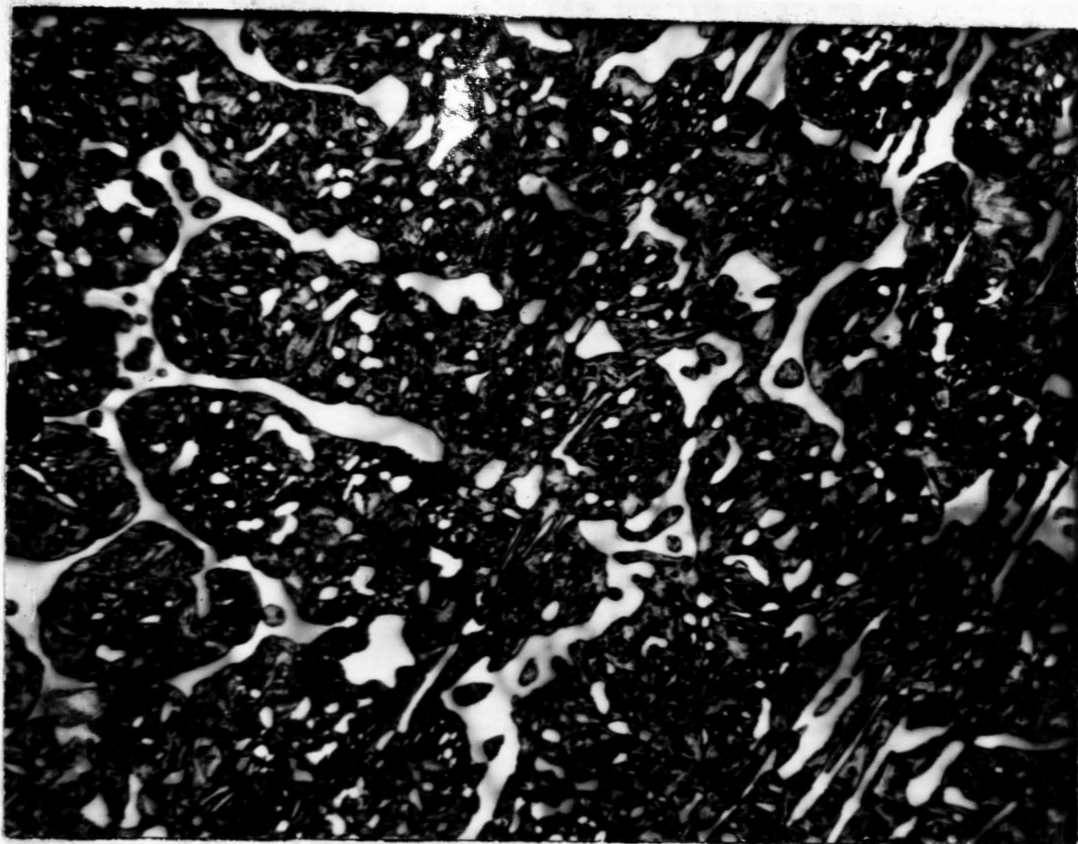
Picral Etch.

No. 25   Annealed at 925° C for 40 minutes   1000 x
Picral Etch.
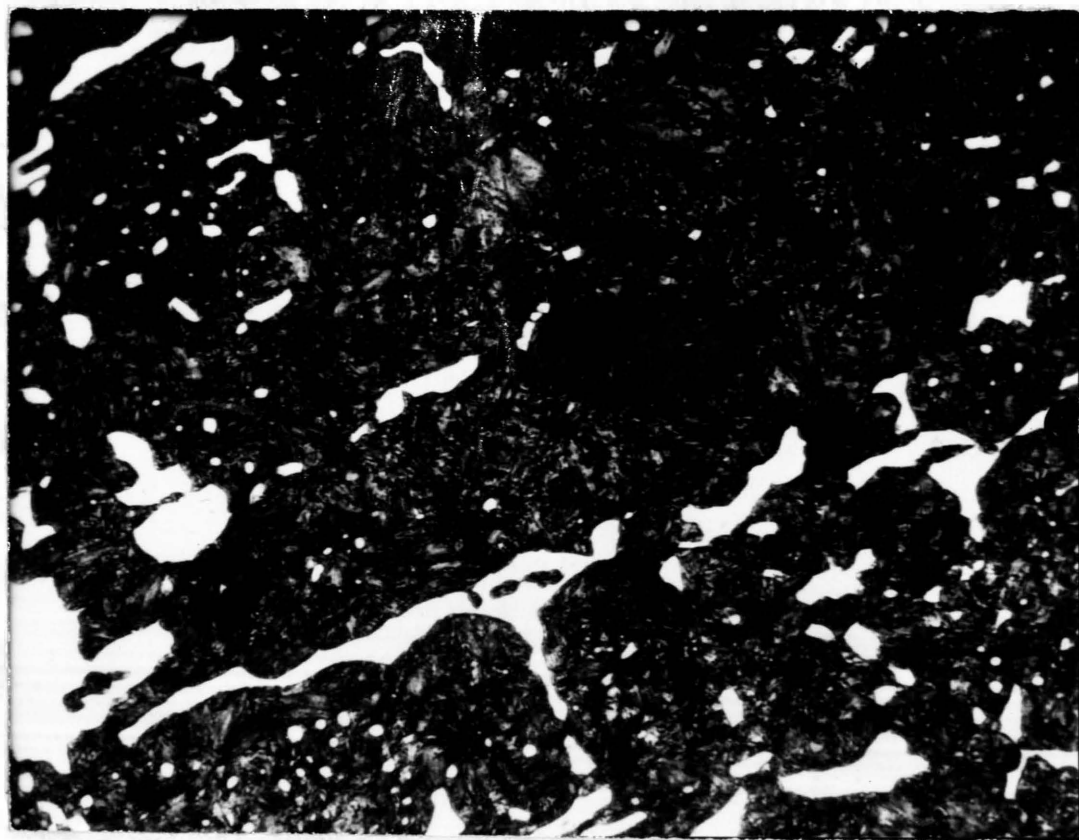
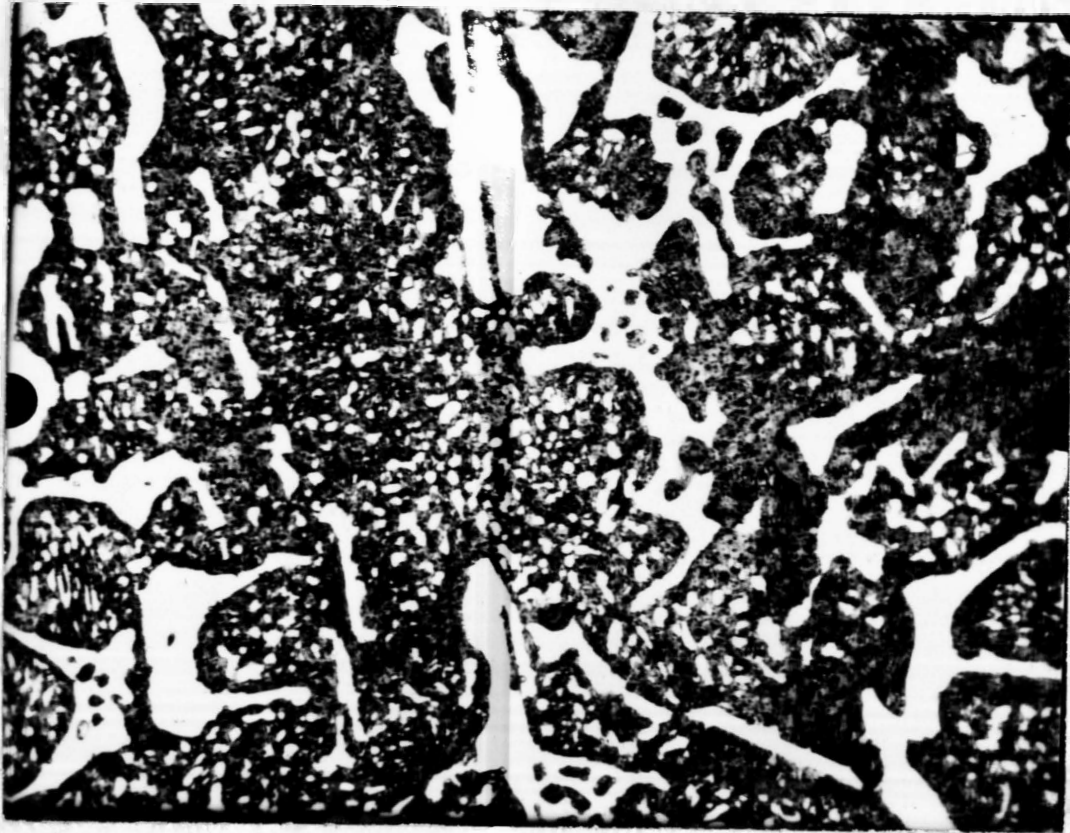No. 26   Annealed at 925° C for 80 minutes   1000 x
Picral Etch.
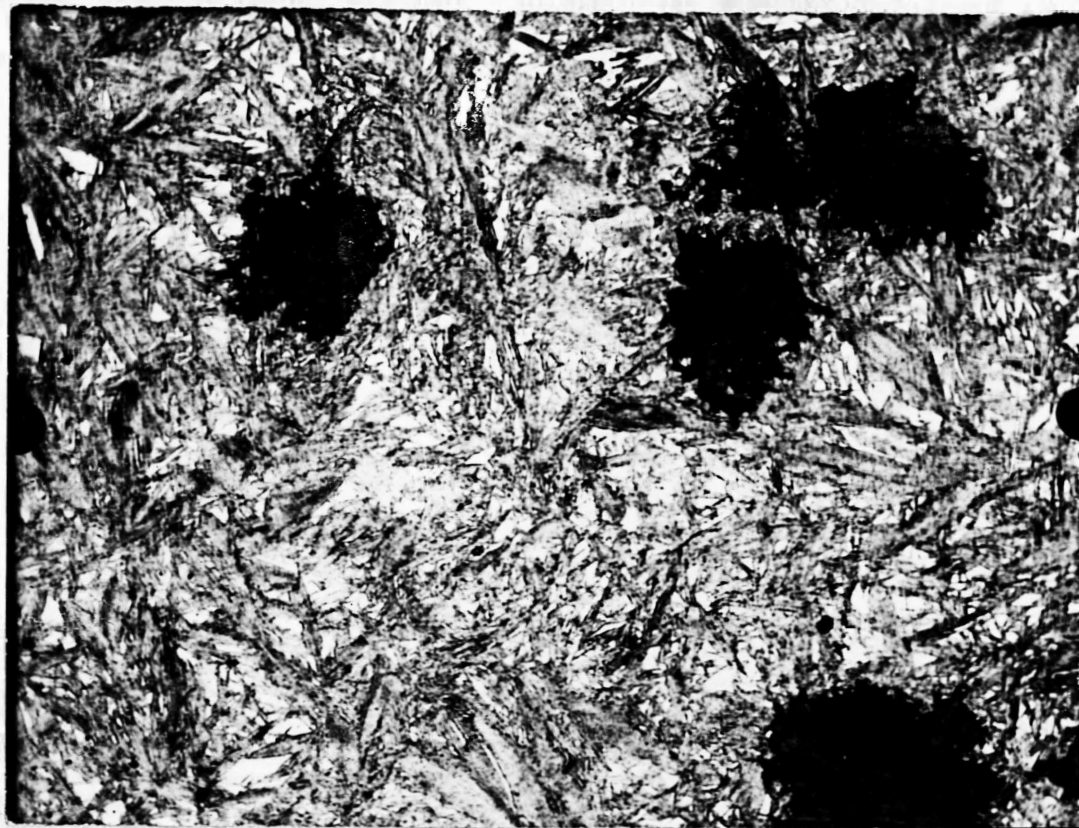
No. 27   Annealed at 925° C for 160 minutes   1000 x
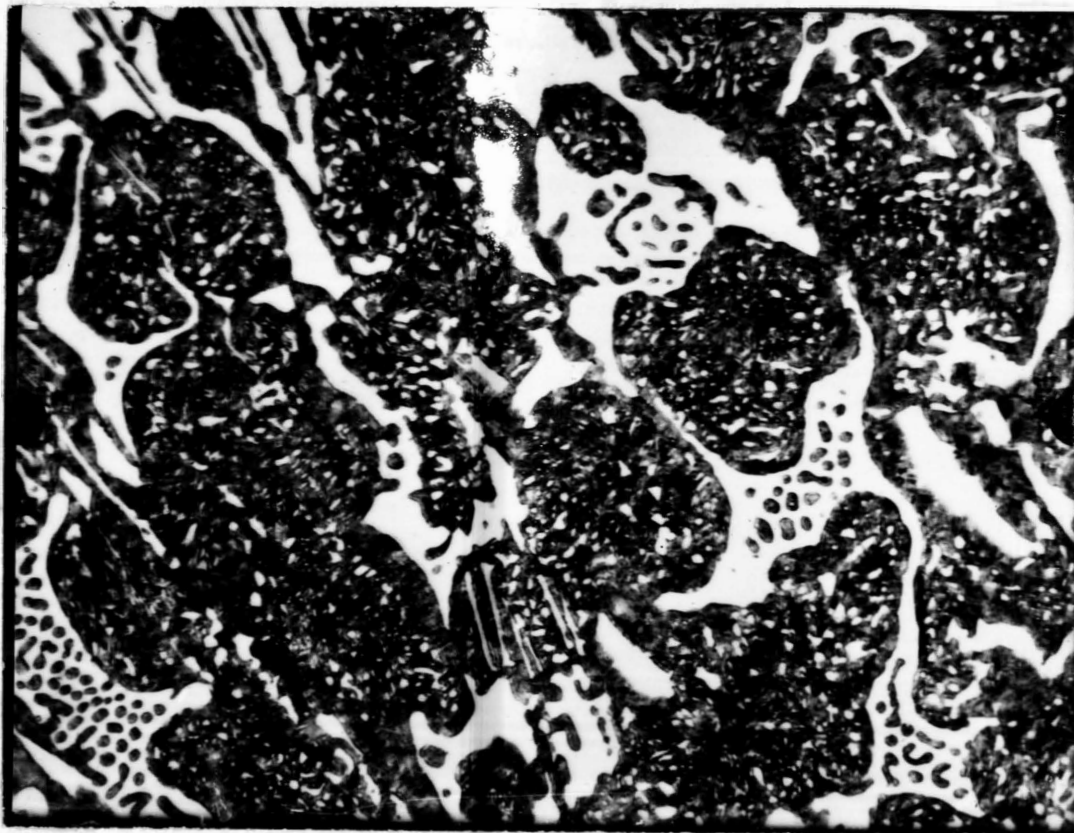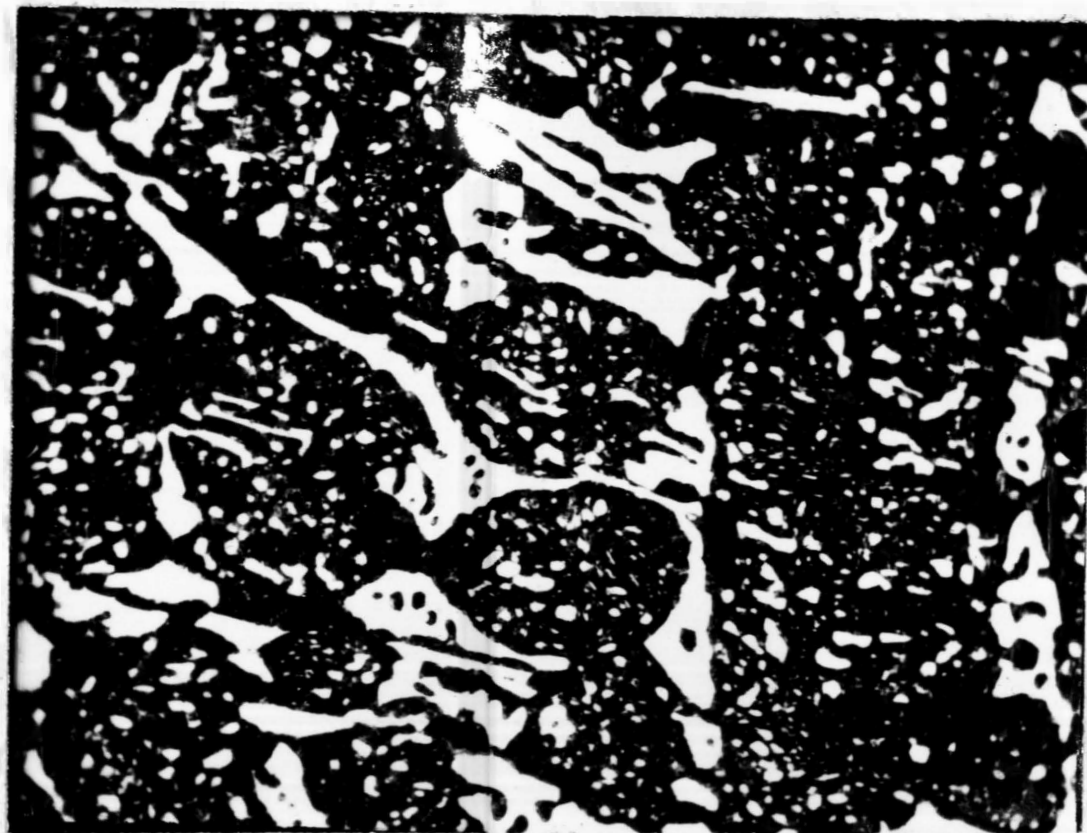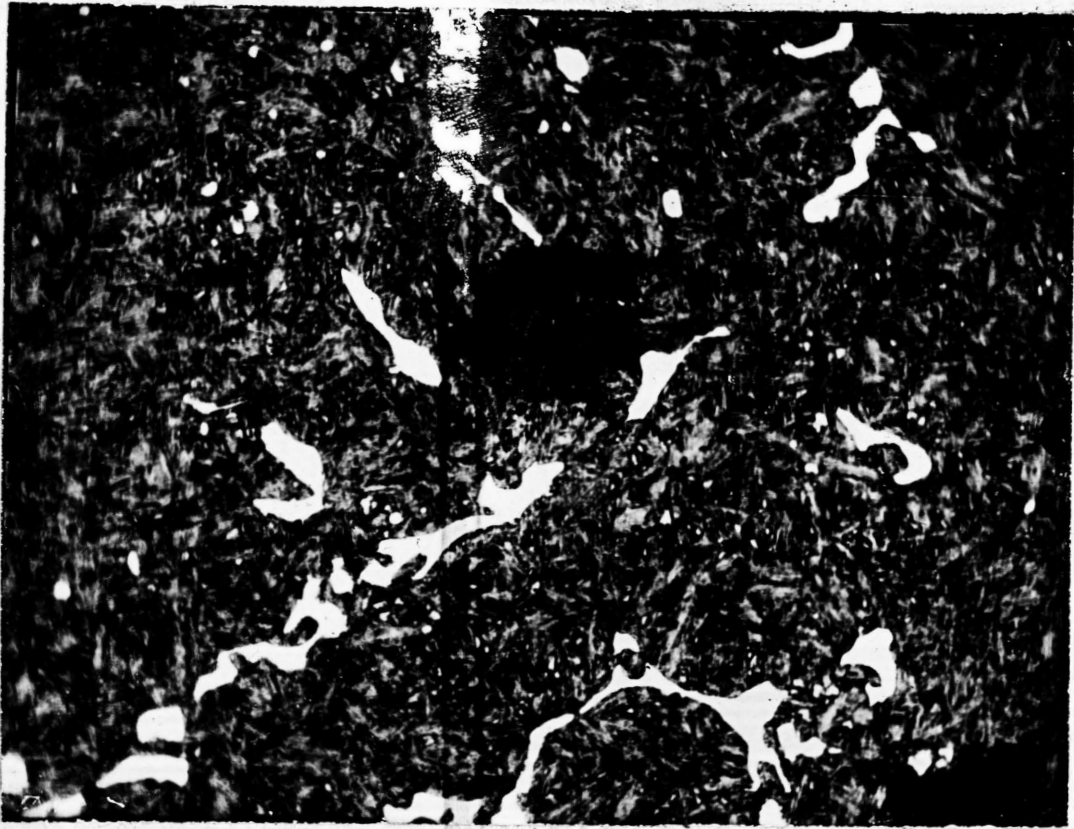
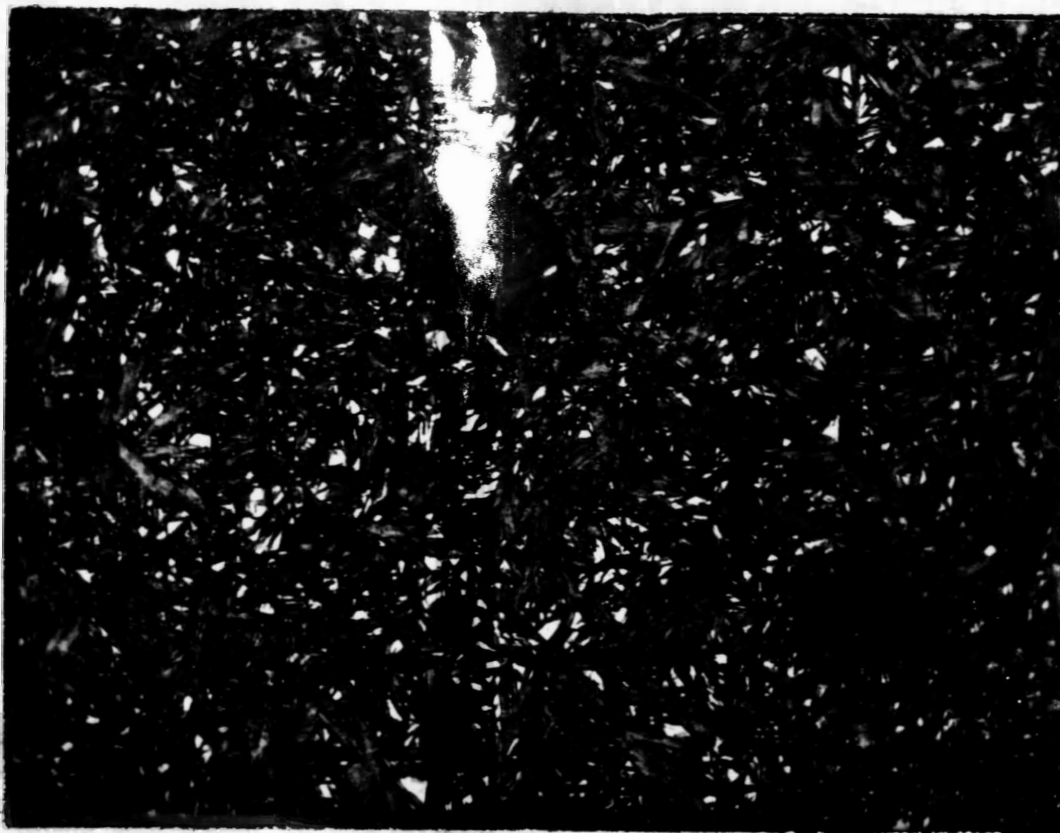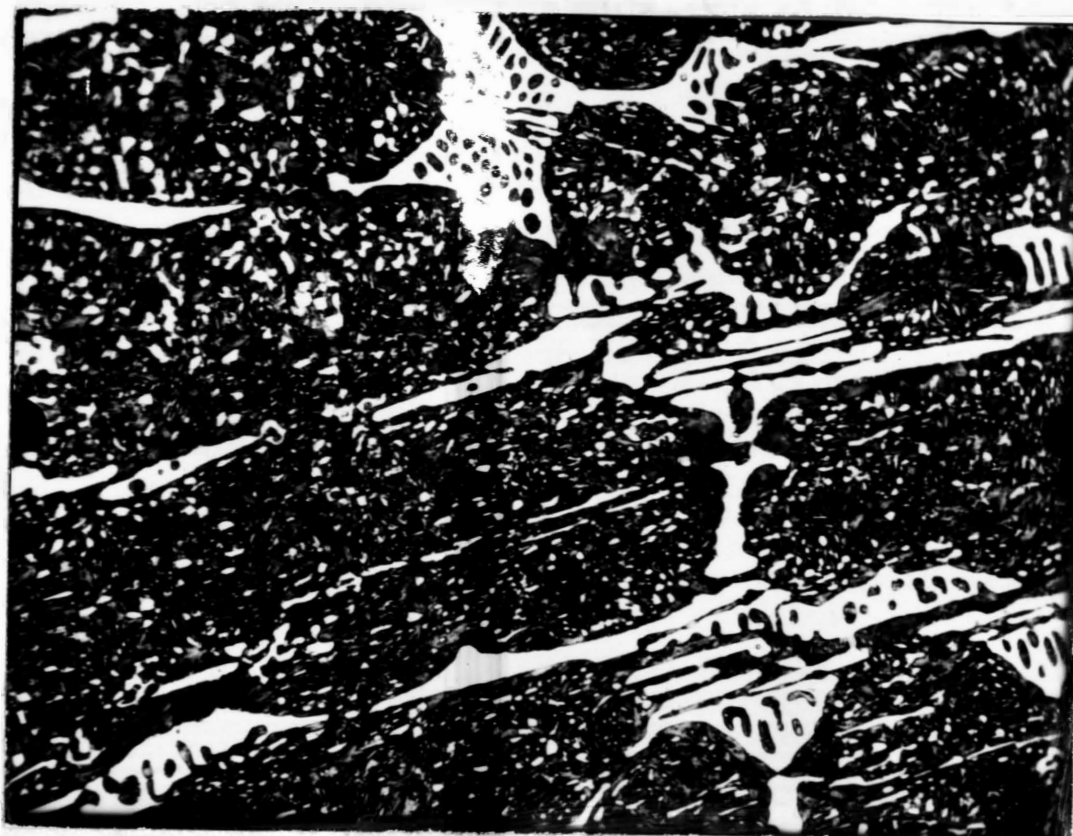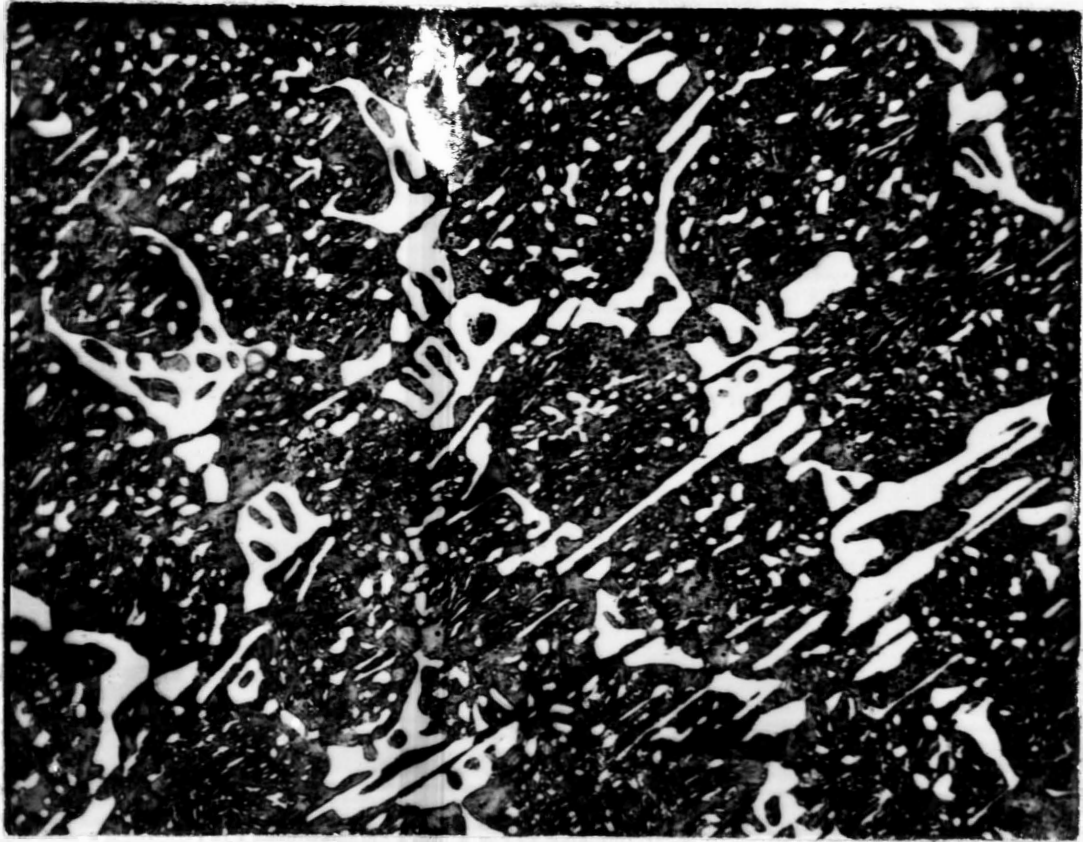Picral Etch.

RESULTS OF METALLOGRAPHIC EXAMINATION

The following points were observed in the examination of the specimens under the microscope.

1. The "as cast" sample showed only primary cementite and pearlite. No spherical carbides were observed. (Micrograph No. 1 page 34).

2. On annealing for short periods of time, it was observed that secondary globular carbides were precipitated in the austenite matrix which grew in size with time. (Micrograph No. 2, 4, 6). The precipitation and growth of the secondary carbides seemed to be at the expense of primary cementite. The primary cementite areas decreased in size during this period. (Micrograph No. 22,23,24).

3. For short periods of time some areas etched darker than the rest of the matrix. Most of the dark etching areas were observed to be around the secondary carbides. (Micrograph No. 9). During this period, no expansion of the specimen was noticed. This indicated that apparently no graphitization had taken place.

4. The graphite nuclei seemed to precipitate along the secondary carbide-austenite interface. In some cases it was observed that the graphite nuclei formed on the primary cementite-austenite interface. (Micrograph No. 6,).

5. The rate of growth of secondary carbides seemed to increse with temperature.

6. The graphitization was complete in a shorter period at higher temperatures.

7. The area in which graphite nodules are formed, gets de-
   pleted of secondary carbides at a faster rate. (Micro-
   graph No. 26,).

DETERMINATION OF ACTIVATION ENERGY

Theoratical Considerations:

If the precipitation of secondary carbides may be considered to proceed by nucleation and growth, "the isothermal reaction curve for such a process would follow a general differential equation of the type:

$$\frac{dy}{dt} = k(a-y)t^m \qquad \text{Equation 1}$$

where: a is total extent of the reaction possible,
        y is the extent of the reaction at time t,
        k is a temperature dependent constant, and
        m is a constant

k reflects the temperature dependence of the reaction rate and follows the usual exponential form:

$$k = A \exp. \left(-\frac{Q}{RT}\right) \qquad \text{Equation 2}$$

where: Q is activation energy in cal/mole,
        T is absolute temperature
        A is a constant
        R is gas constant

The constant, m, determines the form of the isothermal reaction curve and has been used by Zener as a criterion for the shape of the precipitating particle.

In the integral form, Equation 1 becomes

$$\log \log \frac{a}{a-y} = (m \neq 1)\log t \neq \log \frac{k}{2.3} \qquad \text{Equation 3}$$

To evaluate this equation, it is assumed that the change in the precipitate size is proportional to the extent of the reaction and the maximum size of the precipitate corresponds to the completion of the reaction. If $\log \log \frac{a}{a-y}$ is plotted as a function of log t, a straight line with a slope of

(m $\neq$ 1) should be observed[51]."

Experimental values of the constant k can be determined, The activation energy Q can be evaluated by plotting the logarithm of k against 1/T and measuring the slope.

Zener remarked that the activation energy obtained from values of k had dimensions (time) $^{-m} \neq 1$ and, therefore, required adjustment for comparing the activation energies of different reactions. It is usual to obtain the activation energy values with the rate constant having dimensions (time)$^{-1}$.

Experimental Determination of Activation Energy

The rate of growth of spherical carbides at a particular temperature was determined by measuring the diameter of the largest carbide particle found in each of a series of samples reacted for increasing time intervals. The measurements were made on the micrographs with a scale marked to 1/100 inch with the help of magnifying glass having a magnification of 20. In case of carbide particles which were not truly spherical, an average of several sides was taken to be the true diameter. The results of this investigation are given in Table VII. The diameter of the largest carbide particle as a function of time (on log scale) for different temperatures is plotted in figure 5.

In calculating the activation energy, it is assumed that the change in the particle diameter (y) is proportional to the extent of the reaction and the maximum size of the precipitate (a) corresponds to the completion of the reaction. Log log

$\dfrac{a}{a-y}$ and the corresponding values of time t for different

temperature are listed in Table VII. The plot of log log $\dfrac{a}{a-y}$

versus log t for different temperatures is shown in figure 6.
The points fall very closely on a set of parallel straight
lines. The slope (m $\neq$ 1) of these straight lines is determined
and is found to be equal to 0.6.

The value of log k at different temperatures was evaluated
using Equation 3, and these values are listed in Table VIII
along with the reciprocal of the corresponding absolute tem-
peratures. The plot of log k versus 1/T is shown in figure 7.
A straight line passing through nearly all the points is obtain-
ed. The slope of this straight line $\dfrac{d (\log k)}{d (1/T)}$ was accurately
determined and is equal to 3.65×10^3. The activation energy
is calculated as follows:

$$Q = 2.303 \times R \times Slope$$
$$= 2.303 \times 1.987 \times 3.65 \times 10^3$$
$$= 16700 \; Cal/mole$$

This value of activation energy refers to a quantity
with dimensions $(time)^{-0.6}$. On the more usual basis of $(time)^{-1}$,
for the reaction constant, the activation energy is given by

$$\dfrac{16,700}{0.6} = 27,830 \; Cal/mole.$$

The activation energy calculated is of the same order of
magnitude as the activation energy of carbon diffusion in au-
stenite[52]. It may, therefore, be inferred that carbon dif-
fusion is the rate controlling factor for the growth of sec-
ondary carbides.

The proportionality of secondary carbide growth rate to the diameter was based on the theoretical concepts proposed by Zener[31]. From dimensional arguments alone, he showed that the growth coordinate varies with time, t, according to the equation

$$S = \alpha_\lambda (Dt)^{1/2}$$

Equation 4

where α_λ is the growth coefficient and subscript λ refers to the number of dimensions

D is the atomic diffusion coefficient.

S refers to the half width of a plate if the growth of a plate is considered. In the case of a cylinder S is the radius of the cylinder, while it refers to the radius of the particle in considering the growth of a spherical particle.

Zener arrived at his conclusions assuming that the boundary conditions at the interface correspond to

$$n\{t, S(t)\} = n_1$$

Equation 5

where $S(t)$ is the value of s at the interface. In the case of a plate precipitate s is the linear coordinate, while in the case of a spherical precipitate, s is the radial coordinate.

Equation 5 corresponds to the conditions wherein precipitate particles have attained a size large compared to the critical size of a stable nucleus and the rate of growth is limited solely by diffusion.

The final boundary conditions relates the rate of advance

of the interface, $\dot{S}$, to the gradient of the concentration at the interface. Upon equating the rate at which solute atoms are left behind the interface in the precipitate to the rate at which the solute atoms encounter the interface in the matrix, the following equation is obtained.

$$(n_o - n_1)\dot{S} = D\left(\frac{\partial n}{\partial s}\right)_{s=S} \qquad \text{Equation 6}$$

In order to obtain the velocity of advance S, the value of $\frac{\partial n}{\partial s}$ at the interface is estimated and this value is substituted in Equation 6, and then it is solved for the function S(t). In the one dimensional case it leads to the following estimate.

$$\frac{\partial n}{\partial s}\bigg|_{s=S} \simeq \Delta n / \Delta s$$

$$\text{where} \quad \Delta s = 2(n_o - n_a)S/\Delta n \, ,$$

$$\text{and} \quad \Delta n = (n_a - n_1)$$

n_o is the concentration of solute atoms in the precipitate, n_1 is the concentration in the matrix which is in equilibrium with the precipitate and n_a is the concentration in the matrix far away from the precipitate.

Upon substituting this estimate back into Equation 6, and solving for S, we obtain:

$$S \simeq \alpha_1^* (Dt)^{1/2}$$

$$\text{with} \quad \alpha_1^* = \frac{n_a - n_1}{(n_o - n_1)^{1/2}(n_o - n_a)^{1/2}}$$

Zener further stated that the growth coefficient of a spherical particle can be evaluated precisely as in the one dimensional case when the solute atoms are depleted from only a comparatively thin shell surrounding the spherical precipitate. Such treatment leads to the result that

$$\alpha_3^* = 3^{\frac{1}{2}} \alpha_1^*$$

Equation 7

"The quantity α_3^* as given in Equation 7 is a natural parameter in terms of which to express the exact solution of the expanding spherical precipitate."

The shape of curves in Figure 5 depends on the value of m in Equation 1. The curves will be straight lines only when m is unity. In the present case, the value of m is 0.6. The exact shape of the curve in the regions of inflection can only be evaluated if a number of specimens are treated at close intervals of time within that region. Due to the high cost of the preparation of specimens the author was limited to only 28, as compared to the original number of 64 that was first suggested by Dr. D. S. Eppelsheimer.

TABLE VII

Variation of log log $\frac{a}{a-y}$ with time at Various Temperatures

Time in	Carbide particle size in in. x 10^{-5}	a	$\frac{a}{a-y}$	log log $\frac{a}{a-y}$
a. Temperature 800° C				
40	5.5	11.5	1.93	-0.54
80	6.5	11.5	2.45	-0.41
160	9.5	11.5	5.4	-0.14
320	11.5	11.5	10	-0.00
b. Temperature 825° C				
40	7.5	13.5	2125	-0.453
80	9.5	13.5	3.37	-0.280
160	11.5	13.5	6.75	-0.081
320	13.5	13.5	10.00	-0.000
c. Temperature 875° C				
20	10.5	15.0	3.285	-0.2869
80	12.5	15.0	5.75	-0.12
160	15.0	15.0	10.00	-0.000
d. Temperature 925° C				
5.	6.0	16.0	1.6	-0.69
10	8.0	16.0	2.0	-0.52
20	11.0	16.0	3.2	-0.297
40	12.5	16.0	4.57	-0.18
80	16.0	16.0	10.00	0.00

TABLE VIII

Values of $\frac{1}{T}$ and log K at Various Temperatures

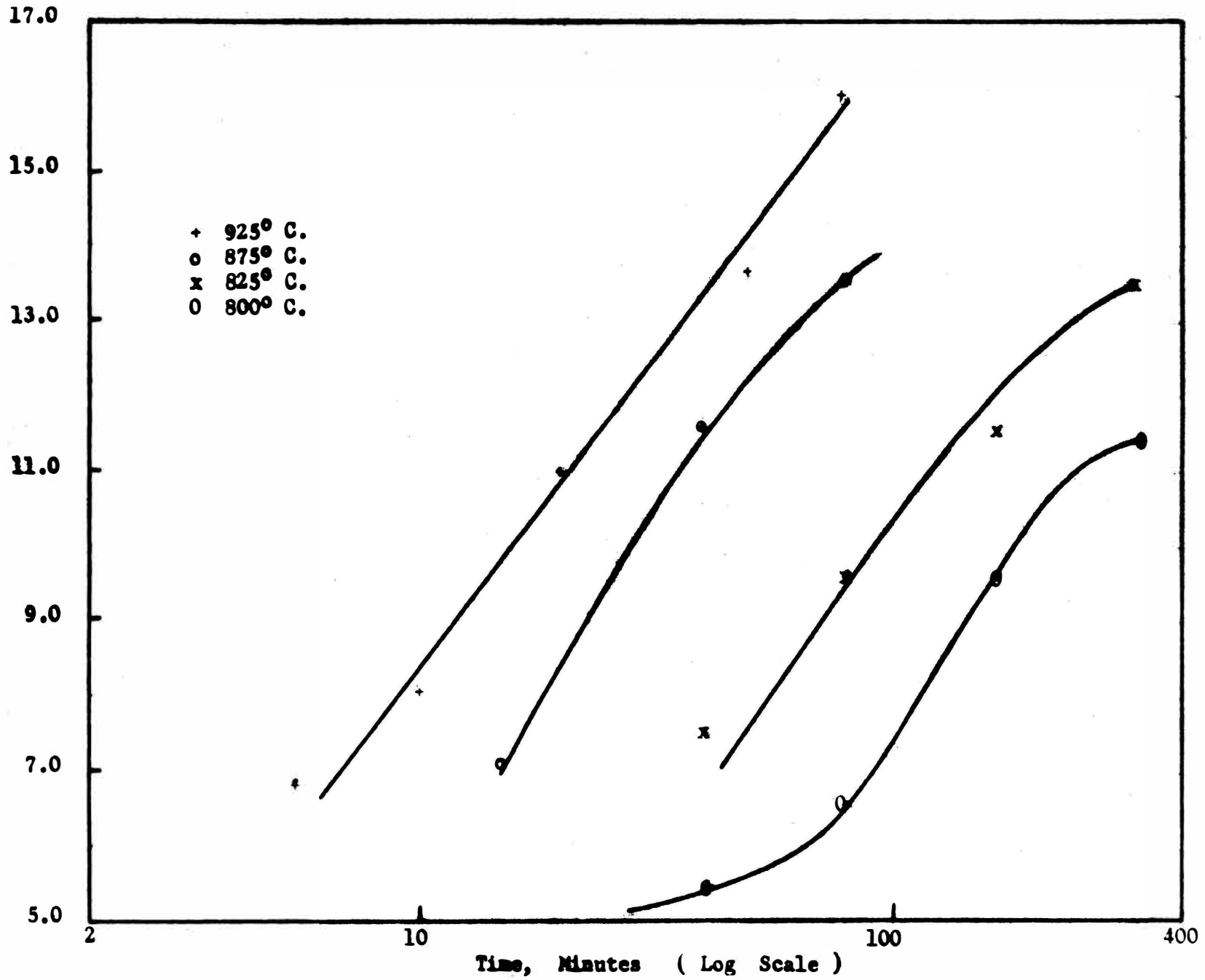| Temperature in $^{\circ}C$	Temperature in $^{\circ}K$	$1/T \times 10^{-5}$	log K
800	1073	93.5	0.0617
825	1098	91.0	0.1417
875	1148	87.0	0.3217
925	1198	83.6	0.4217

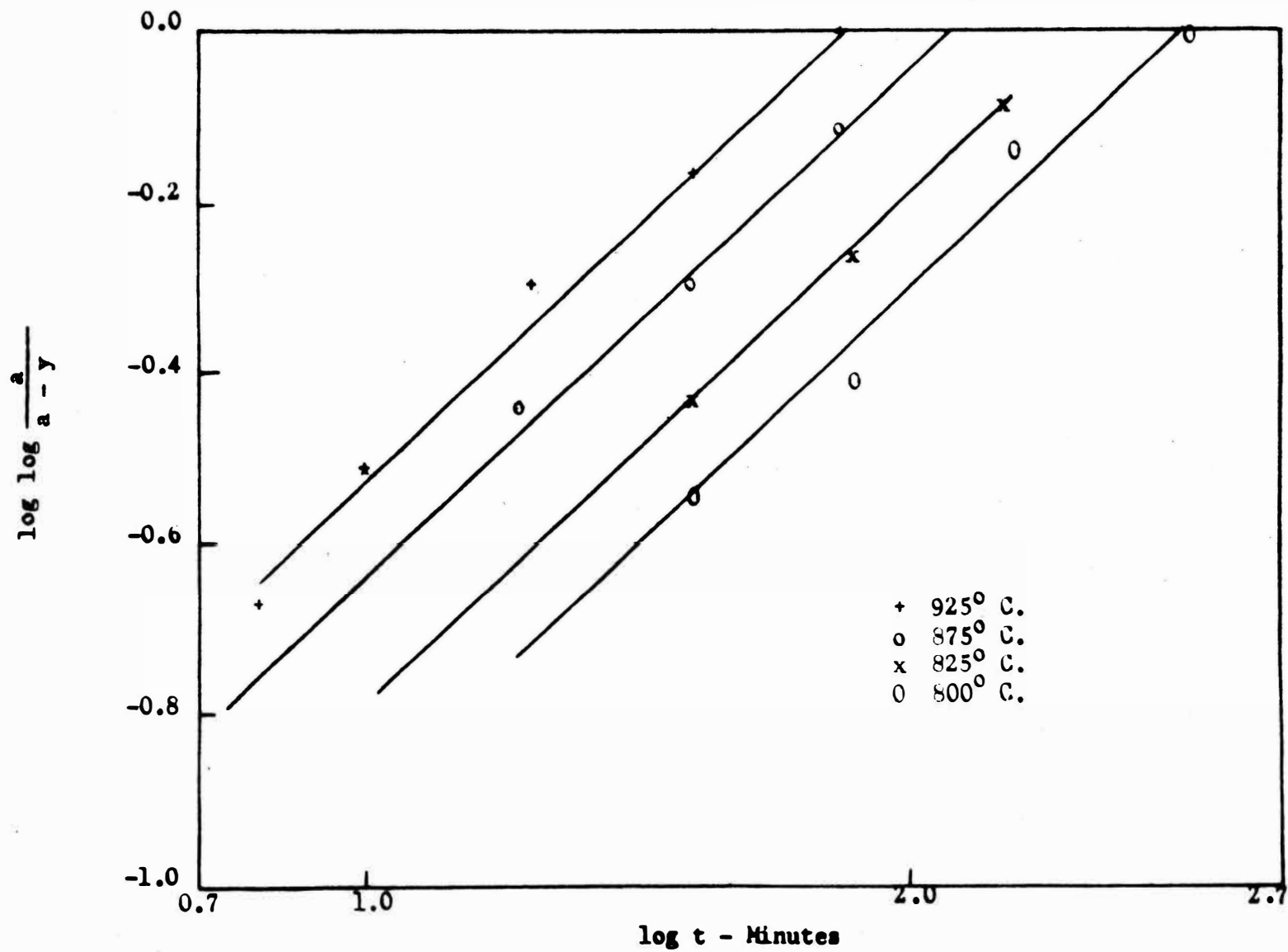Figure 5 — GROWTH CURVES OF SECONDARY CARBIDES AT VARIOUS TEMPERATURES

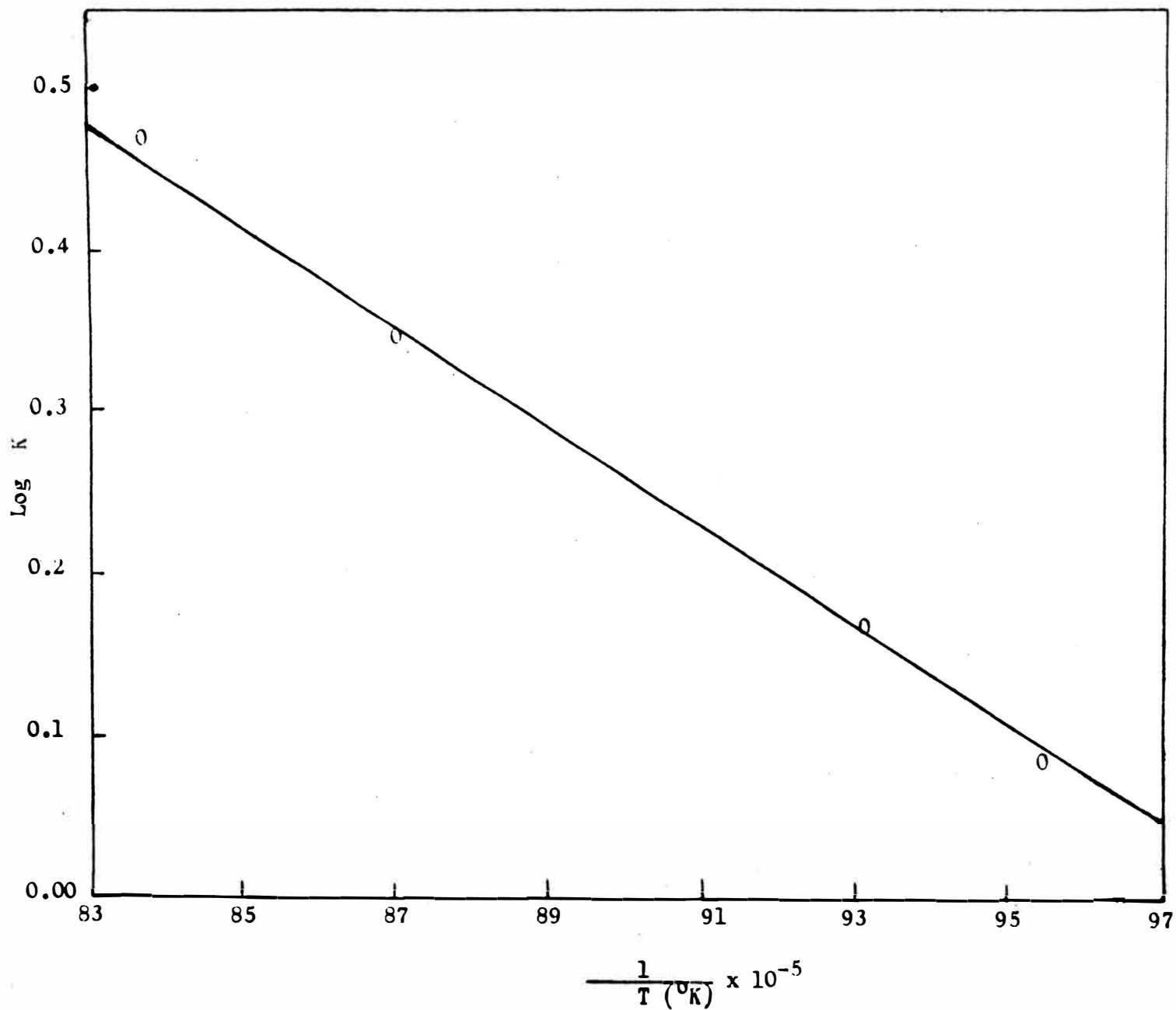Figure 6 – GRAPH OF $\log \log \dfrac{a}{a-y}$ vs. log t

Figure 7 - GRAPH OF Log K VS. $\frac{1}{T}$

Possible Errors

It was assumed in the present investigation that the largest particle measured was cut through the center of the spherical particle by the plane of the sample. The probability of cutting some of the largest particles through the center increases with the number of particles. In most of the photomicrographs, a sufficient number of carbide particles were present to assume that some of the particles were cut through the center. On an average the diameter of ten largest particles was measured and the diameter of these particles was sufficiently in agreement to indicate that these were probably cut through the center.

The small scatter of points in Figures 6 and 7 indicates that the error involved in activation energy measurement is not greater than that of methods employed for activation energy determination. In the present case it is difficult to evaluate the percentage error involved.

Besides the diffusion of carbon, the other diffusion processes taking place are diffusion of iron and silicon atoms. The activation energy of iron and silicon diffusion through austenite is more than 60,000 cal/mole.[53] Therefore, if it is assumed that the percentage error in the activation energy calculation is 20%, the value of activation energy calculated is 27,800 cal/mole, which is in fair agreement with the value of 23,000 cal/mole obtained by extrapolating the results of Wells, Batz and Mehl for the diffusion of carbon through austenite.

Suggestions for Further Work:

The activation energy of secondary carbide precipitation can be very accurately determined, if the secondary carbides are electrolytically extr_cted and weighed from samples which have been annealed for various intervals of time at different temperatures. The chief difficulty which may be encountered in such a work is the separation of secondary carbides from primary cementite and other inclusions that may be present such as oxides, silicates, and sulphides. The problem offers further difficulties when temper carbon is precipitated. Also great care will have to be excercised to see that no reduction of size takes place due to dissolution of the carbides.

The kinetics of seconary carbide precipitation in white cast irons containing various amounts of different alloying elements should be investigated. This may give an insight into the role played by alloying elements during graphitization. The composition of the secondary carbides might be evaluated by taking x-ray diffraction photographs of the electrolytically extracted carbides.

DISCUSSION OF EXPERIMENTAL RESULTS

It is observed that secondary carbides are not present in the "as cast" condition and, therefore, it may be inferred that these are precipitated during the initial stages of annealing. The decrease in the amount of primary cementite during this period gives an indication that the precipitation and growth of secondary carbides take place at the expense of primary cementite.

The dark etching areas formed before any change in length is noticed, may be due to the precipitation of submicroscopic amounts of carbon which is coherent with the secondary carbide lattice.

As graphite nodules are found at the austenite-cementite into interfaces, it was assumed by previous investigators [25], [27], [32] that the graphite nuclei form at these interfaces. The formation of graphite nodules within the austenite grain was never clearly explained, except by a vague statement [49] that the conditions at the cementite-austenite interface are not favourable for the nucleation of graphite. On the other hand, if it is assumed that the graphite nuclei form at the austenite-secondary carbide interface, as shown in the present investigation, the explanation for the formation of graphite nodules within the austenite region becomes very simple. The formation of most of the graphite nodules at the austenite cementite interface may be due to the high concentration of carbon in this area, which results in faster rate of precipitation and growth of secondary carbides in this region.

On the basis of chemical analysis, Schwartz[49] reported that carbide in malleable iron has silicon associated with it. Similar conclusions were drawn by Hatfield[39] earlier. But it was shown by Owen[50] that silicon is not present in the cementite lattice. The results of Owen are based on the x-ray diffraction work, and in the opinion of the author, his studies were confined to primary cementite only which does not contain silicon in its lattice. The secondary carbides may have silicon associated with them, and the results of Hatfield and Schwarts confirm this assumption.

The role of alloying elements may be explained, if the secondary carbides are extracted and analysed by x-ray diffraction technique to know whether the alloying elements enter the secondary carbide lattice. The kinetics of secondary carbide precipitation and growth in the presence of different alloying elements may also give an insight to the role played by alloying elements during graphitization.

CONCLUSIONS

1. The precipitation of secondary carbides during the early stages of annealing has been definitely proved. (Figure 2, p. 35).

2. The secondary carbides grow to a maximum size, after which these decompose into temper carbon and carbon depleted austenite. (Micrograph 6, p. 39).

3. The rate of growth and the maximum size of the secondary carbide increase with the temperature.

4. The graphite nuclei are formed at the austenite secondary carbide interface. (Micrograph 6, p. 39).

5. The activation energy of growth of secondary carbide is 27,800 cal/mole. (p. 65). This value is of the same order of magnitude as the diffusion of carbon in austenite. Therefore, it may be inferred that the rate of secondary carbide growth is controlled by the diffusion of carbon through austenite.

6. The following mechanism of graphitization of Fe-C-Si alloy is proposed.

    (a) On heating the Fe-C-Si alloy to the annealing temperature, an equilibrium between austenite and primary cementite is attained.

    (b) The globular secondary carbides are precipitated in the austenite matrix. (Micrographs 2, 4, 6).

    (c) The equilibrium between primary cementite and austenite is disturbed. Some amount of primary cementite goes into solution, and the secondary carbides

grow in size.

(d) On attaining the maximum size, the secondary carbides decompose into graphite and carbon depleted austenite.

(e) Some more primary cementite is taken into solution.

(f) This process, of solution of primary cementite, precipitation and growth of secondary carbides and their decomposition, goes on until the austenite conta the equilibrium amount of carbon for the temperature.

BIBLIOGRAPHY

1. A. Taub, The Mechanism of Graphitization, <u>Foundry.</u> Oct. 1958, p. 82.

2. A. E. Hammer; Referred in H. A. Schwartz: <u>American Malleable Cast Iron,</u> The Penton Publishing Co. 1922, p. 27.

3. A. A. Pope: Ibid, p. 29.

4. A. Sauveur, Microstructure of Steel, <u>Trans., AIME,</u> vol. 26, 1896, p. 866.

5. Charpy and Grent: On the Equalibrium of Iron-Carbon Systems, <u>Engineering</u> (London) vol. 73. P. 262.

6. H. Howe: The Iron-Carbon Diagram, <u>Transaction, AIME,</u> vol. 39. 1908, p. 3.

7. R. Moldenke: <u>The Production of Malleable Castings,</u> The Penton Publishing Co. 1910.

8. W. H. Hatfield: Decarburization of Iron-Carbon alloys, <u>Engineering,</u> vol. 87. 1910, p. 801.

9. O. Ruff and O. Goecke: The solubility of Carbon in Iron, <u>Metallurgie,</u> vol. 8, 1911, p. 417.

10. R. Ruer and N. Iljin: The Stable Iron-Carbon System, <u>Metallurgie,</u> vol. 8. 1911, p. 97.

11. O. W. Storey: A Study of the Annealing Process for Malleable Castings, <u>Metallurgical and Chemical Engineering,</u> vol. 12. 1913, p. 383.

12. P. D. Merica and L. J. Gurevich: Notes on the Graphitization of White Cast Iron upon Annealing, <u>Bureau of Standards Technical Paper 129,</u> vol. 12. 1919.

13. K. Honda and T. Murakami: On Graphitization of Iron-carbon alloys, J. Iron Steel Inst., vol. 102. 1920, p. 287.

14. P. Pingault: The Formation and Decomposition of Cementite, C. R. Acad. Sci., Paris, vol. 1930. P. 1007.

15. E. C. Bain: On the Rates of Reactions in Solid Steel, <u>Trans., AIME,</u> vol. 20, 1932. P.385

16. A. Philips and E. S. Davenport: Malleablizing of White Cast Iron, <u>Trans., AIME,</u> vol. 67. 1922, p, 466.

17. A. Hays and W. J. Diedrichs: The Mechanism for the Graphitizatic of White Cast Iron and its Application of Malleablization, <u>Bulletin 71,</u> Iowa State College. 1924

18. H. A. Schwartz: Present Theories on Graphitization, Foundry, Vol. 56. 1928, p. 871.

19. E. C. Bain: op. cit., 14.

20. C. Yap: The Free Energy, Entropy and Heat of Formation of Iron Carbide, Trans., Faraday Society, No. 138, vol. 28. 1932.

21. H. A. Schwartz: The Metastability of Cementite, Trans., ASM, vol. 23. 1935, p. 126.

22. J. Chipman: Ibid, Discussion, p. 135.

23. C. Wells: Graphitization of High Purity Iron-carbon Alloys, Trans., ASM, vol. 26. 1938, p. 289.

24. A. Sauveur and H. L. Anthony: Malleable Castings, Trans., ASM, vol. 23. 1935, p. 409.

25. H. A. Schwartz: Nucleation of Graphite by Manganese Sulphide, Metals and Alloys, vol. 6. 1935, p. 328.

26. H. A. Schwartz and W. Ruff: Origin and Growth of Graphite Nuclei in Solid and Liquid Iron Solution, Trans., AIME, vol. 120. 1936, p. 217.

27. C. Wells: op. cit., 23.

28. H. A. Schwartz: The Kinetices of Graphitization in White Cast Iron Trans., ASM, vol. 30. 1942, p. 1928.

29. H. A. Schwartz: The Principles of Graphitization, Trans., AFS, vol. 50. 1942, p. 1.

30. W. D. Mc Millan: The Effect of Composition on the Annealing of White Cast Iron, Ibid, 30.

31. C. Zener: Theory of Growth of Spherical Precipitates from Solid Solutions, J. Applied Physics, vol. 20. 1949, p. 950

32. B. F. Brown and M. F. Hawkes: Kinetics of Graphitization of Cast Iron, Trans., AFS, vol. 59. 1951, p. 181.

33. W. D. Mc Millan: op. cit., 30.

34. F. Burke and W. S. Owen: Kinetics of First Stage Graphitization in Fe-C-Si Alloys, J. Iron Steel Inst., vol. 176. 1954, p. 147.

35. A. Hultgren and G. Ostberg: Structural Changes during Annealing of White Cast Irons of High S:Mn Ratios, J. Iron Steel Inst., vol. 176. 1954, p. 351.

36. H. A. Schwartz: Some New Aspects of Iron-carbon Diagram, Trans., Am. Soc. Steel Treat., vol. 19. 1932, p. 403.

37. F. Wust and O. Petersen: Influence of Silicon upon the Iron-carbon System, Metallurgy, vol. 3. 1906, p. 811.

38. M. I. Becker: Equlibrium at H igh Temperatures in the Iron-carbon silicon System, J. Iron Steel Inst., vol. 112. 1925, p. 239.

39. W. H. Hatfield: Cast Iron in the Light of Recent Researches Charles Griffin & Co., Ltd., London. 1928.

40. H. A. Schwartz: op. cit., 29.

41. B. E. Brown and M. F. Hawkes: op. cit., 32.

42. J. B. Austin: The Effect of Changes in Condition of Carbide on Some Properties of Steel, Trans., ASM, vol. 38.

43. F. Burke and W. S. Owen: op. cit., 32.

44. H. A. Schwartz: op. cit., 29.

45. C. Wells, W. Batz and R. F. Mehl: Diffusion coefficient of Carbon in Austenite, Trans., AIME, vol. 188. 1950, p. 553.

46. F. Burke and W. S. Owen: op. cit., 34.

47. B. F. Brown and M. F. Hawkes: op. cit., 32.

48. F. Burke and W. S. Owen: op. cit., 34.

49. H. A. Schwartz: Chemical Composition of Iron, Trans. AFS, vol. 54. 1946, p. 101.

50. W. S. Owen: The Carbide Phase in Iron-Carbon-Silicon Alloys, J. Iron Steel Inst., vol. 167. 1951, p. 117.

51. R. W. Balluff, M. Cohen and B. L. Aoerback: Ther Tempering of Chromium Steels, Trans. ASM, vol. 43. 1951, p. 497.

52. C. Wells, W. Batz and R. F. Mehl, op. cit., 45.

APPENDIX

It has been suggested by Dr. J. L. Kassner that a curve between the particle size and the number of particles in the immediate neighbourhood of largest particle size should be drawn. If the curves corresponds to curve (1) in Figure 8, the straight line portion should be extrapolated as shown in the figure and t he largest particle size should be taken corresponding to its intercept an the x-axis. If the curve corresponds to curve (2) in Figure 8, the largest particle cannot be taken for calculation of activation energy.
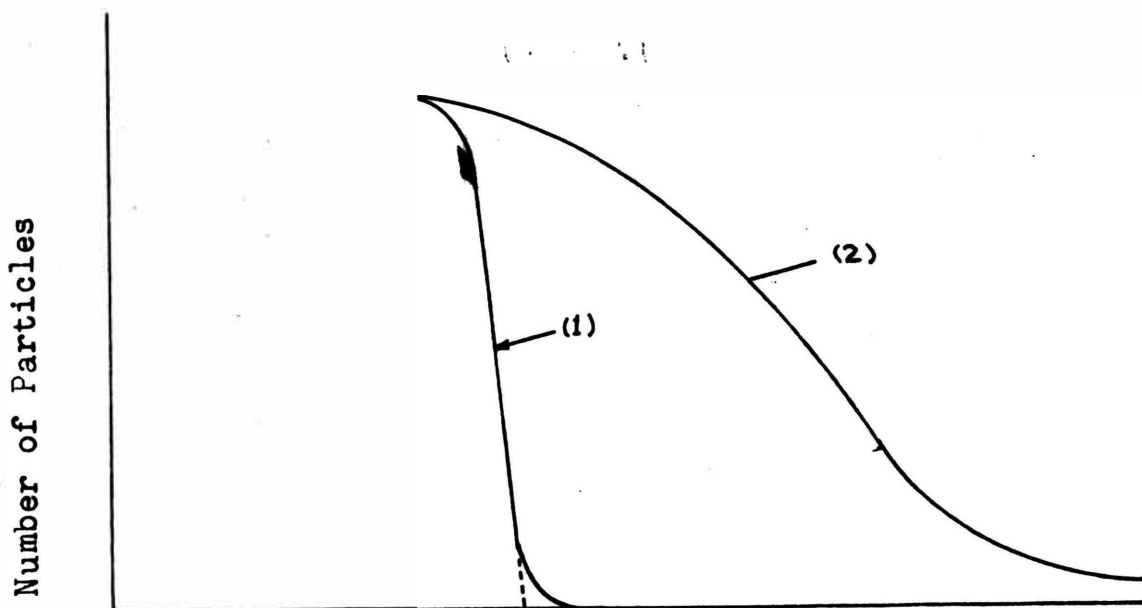
Figure 8   Diameter of particle

VITA

The author was born on April 9, 1932, at Rawalpindi, India. He attended N. Wadia College at Poona. He received a Bachelor of Science Degree in Metallurgical Engineering from Banaras Hindu University in 1957. From July, 1957 to August, 1958, he was employed as a lecturer in Metallurgical Engineering at Banaras Hindu University. He joined the Missouri School of Mines and Metallurgy in September, 1958.